



OPEN ACCESS

EDITED BY

Nathan Alder,
University of Connecticut, United States

REVIEWED BY

Dejana Mokranjac,
Ludwig Maximilian University of Munich,
Germany
Richard Rachubinski,
University of Alberta, Canada

*CORRESPONDENCE

Ralf Erdmann,
✉ ralf.erdmann@rub.de
Vishal C. Kalel,
✉ vishal.kalel@rub.de

RECEIVED 28 April 2023

ACCEPTED 03 August 2023

PUBLISHED 17 August 2023

CITATION

Krishna CK, Schmidt N, Tippler BG,
Schliebs W, Jung M, Winklhofer KF,
Erdmann R and Kalel VC (2023),
Molecular basis of the glycosomal
targeting of PEX11 and its mislocalization
to mitochondrion in trypanosomes.
Front. Cell Dev. Biol. 11:1213761.
doi: 10.3389/fcell.2023.1213761

COPYRIGHT

© 2023 Krishna, Schmidt, Tippler,
Schliebs, Jung, Winklhofer, Erdmann and
Kalel. This is an open-access article
distributed under the terms of the
[Creative Commons Attribution License
\(CC BY\)](https://creativecommons.org/licenses/by/4.0/). The use, distribution or
reproduction in other forums is
permitted, provided the original author(s)
and the copyright owner(s) are credited
and that the original publication in this
journal is cited, in accordance with
accepted academic practice. No use,
distribution or reproduction is permitted
which does not comply with these terms.

Molecular basis of the glycosomal targeting of PEX11 and its mislocalization to mitochondrion in trypanosomes

Chethan K. Krishna¹, Nadine Schmidt¹, Bettina G. Tippler¹,
Wolfgang Schliebs¹, Martin Jung², Konstanze F. Winklhofer³,
Ralf Erdmann^{1*} and Vishal C. Kalel^{1*}

¹Department of Systems Biochemistry, Institute for Biochemistry and Pathobiochemistry, Faculty of Medicine, Ruhr University Bochum, Bochum, Germany, ²Department of Medical Biochemistry and Molecular Biology, Saarland University, Homburg, Germany, ³Department Molecular Cell Biology, Institute of Biochemistry and Pathobiochemistry, Faculty of Medicine, Ruhr University Bochum, Bochum, Germany

PEX19 binding sites are essential parts of the targeting signals of peroxisomal membrane proteins (mPTS). In this study, we characterized PEX19 binding sites of PEX11, the most abundant peroxisomal and glycosomal membrane protein from *Trypanosoma brucei* and *Saccharomyces cerevisiae*. *Tb*PEX11 contains two PEX19 binding sites, one close to the N-terminus (BS1) and a second in proximity to the first transmembrane domain (BS2). The N-terminal BS1 is highly conserved across different organisms and is required for maintenance of the steady-state concentration and efficient targeting to peroxisomes and glycosomes in both baker's yeast and *Trypanosoma brucei*. The second PEX19 binding site in *Tb*PEX11 is essential for its glycosomal localization. Deletion or mutations of the PEX19 binding sites in *Tb*PEX11 or *Sc*PEX11 results in mislocalization of the proteins to mitochondria. Bioinformatic analysis indicates that the N-terminal region of *Tb*PEX11 contains an amphiphilic helix and several putative TOM20 recognition motifs. We show that the extreme N-terminal region of *Tb*PEX11 contains a cryptic N-terminal signal that directs PEX11 to the mitochondrion if its glycosomal transport is blocked.

KEYWORDS

peroxisome, glycosome, peroxin, PEX19, PMP, mPTS, MTS

1 Introduction

Peroxisomes are single membrane bound organelles performing a wide range of functions (Rhodin, 1954; De Duve and Baudhuin, 1966). Glyoxysomes in plants, Woronin bodies in fungi, and glycosomes in trypanosomatid parasites are specialized forms of peroxisomes (Reichle and Alexander, 1965; Breidenbach and Beever, 1967; Opperdoes and Borst, 1977). Peroxisomes can multiply by growth and division, or they can form *de novo* from pre-peroxisomal vesicles that are supposed to bud from the endoplasmic reticulum (Hoepfner et al., 2005; Motley and Hetteema, 2007). Peroxisomes import matrix as well as membrane proteins post-translationally (Goldman Blobel, 1978; Lazarow and Fujiki, 1985; Sacksteder et al., 2000; Jones et al., 2004). The import depends on a machinery of Peroxins (PEX proteins) and requires the presence of peroxisomal targeting signals in the cargo

proteins (Gould et al., 1989; Swinkels et al., 1991; Faber et al., 1995). Biogenesis of peroxisomes requires two distinct machineries for protein targeting: The first is responsible for the formation of the peroxisomal membrane by the targeting and insertion of peroxisomal membrane proteins (PMPs), and the second machinery is responsible for the import of peroxisomal matrix proteins (reviewed in (Agrawal and Subramani, 2016)). The trafficking of proteins destined for the peroxisome matrix has been well studied. A striking feature is that peroxisomes can import folded, even oligomeric proteins (McNew and Goodman, 1994; Leon et al., 2006). Peroxisomal matrix proteins contain type 1 or type 2 peroxisomal targeting signals (PTS1/PTS2) at the extreme C-terminus or close to the N-terminus, respectively (Gould et al., 1989; Swinkels et al., 1991; Faber et al., 1995). Some proteins contain internal targeting signals (Galland et al., 2010) and some are transported by piggy-backing onto a PTS-containing protein (Islinger et al., 2009). The import of peroxisomal matrix proteins depends on cycling receptors that recognize peroxisomal proteins via their PTS in the cytosol and target them to a docking complex at the peroxisomal membrane. Import takes place through a transient pore or hydrogel-filled pore in an unknown fashion (Erdmann and Schliebs, 2005; Meinecke et al., 2016; Gao et al., 2022). The cargo-unloaded receptors are mono-ubiquitinated and released to the cytosol for another round of import in an ATP-dependent manner by the peroxisomal exportomer (Platta et al., 2004; Platta et al., 2005). The machinery that is responsible for the topogenesis of membrane proteins is distinct from the import machinery for matrix proteins (Reviewed in (Hasan et al., 2013; Mayerhofer, 2016)). Only three peroxins with a direct role in PMP targeting have been identified, namely, PEX3 (Hettema et al., 2000), PEX16 in mammals (South and Gould, 1999; Sacksteder et al., 2000), and PEX19 (Sacksteder et al., 2000) (Also reviewed in (Kalel and Erdmann, 2018)). In cells lacking any of these proteins, PMPs are either degraded or mistargeted to other subcellular compartments such as mitochondria, endoplasmic reticulum (ER), and membranes of unknown origin (Ghaedi et al., 2000; Hettema et al., 2000; Sacksteder et al., 2000). PMPs contain multiple binding sites (BSs) for the cytosolic receptor and chaperone PEX19 (Jones et al., 2004). These binding sites are essential for targeting of the PMPs to the peroxisomal membrane, as they can function as mPTS i.e., membrane peroxisome targeting signal (Halbach et al., 2005). The mPTS often comprises part of the transmembrane domains and a short adjacent sequence, which contains either a cluster of basic residues or a mixture of basic and hydrophobic amino acids (Marshall et al., 1996) (Reviewed in (Baerends et al., 2000; Murphy et al., 2003; Van Ael and Fransen, 2006)). Rottensteiner et al., developed PEX19 binding site prediction methodology using peptide arrays (Rottensteiner et al., 2004). Unlike PTS1 and PTS2 signals, which can be predicted more reliably (Kamoshita et al., 2022; Kunze, 2023), PEX19 BSs are comparatively degenerate and can be present multiple times in a PMP. Therefore, an efficient PEX19BS predictor is still needed. Nonetheless, PEX19 binding sites (BSs) have been identified in various yeast, human and parasite PMPs, which shows evolutionary conservation across eukaryotes (Rottensteiner et al., 2004; Saveria et al., 2007). In most eukaryotes, PEX19 harbors a farnesylation motif (CaaX box), and farnesylation has been shown to increase the binding

efficiency of PMPs (Rucktaschel et al., 2009). However, trypanosomatid parasite PEX19 proteins lack such a CaaX motif (Banerjee et al., 2005).

PEX11 is an integral peroxisomal membrane protein with at least two predicted alpha-helical transmembrane domains and both termini facing the cytosol (Abe et al., 1998b; Lorenz et al., 1998; Anton et al., 2000; Bonekamp et al., 2013). In the yeast *Saccharomyces cerevisiae*, Pex11p, Pex25p, and Pex27p are the three members of the PEX11 protein family (Erdmann and Blobel, 1995; Rottensteiner et al., 2003; Tam et al., 2003). Similarly, mammals also encode three PEX11-family proteins namely, PEX11 α , PEX11 β , and PEX11 γ (Li and Gould, 2002; Koch et al., 2010). In plants, there are five PEX11 homologs, for e. g., in *Arabidopsis thaliana* AtPEX11a, -b, -c, -d, and -e (Lingard and Trelease, 2006). PEX11 family proteins are involved in the proliferation of peroxisome in yeasts, plants, and mammals (Erdmann and Blobel, 1995; Abe and Fujiki, 1998a; Schrader et al., 1998; Orth et al., 2007; Koch et al., 2010). Deletion of PEX11 in yeast has an effect on the β -oxidation of fatty acids, which can be due to defects in the transport of metabolites across the peroxisomal membrane (Sulter et al., 1993). PEX11 β is widely expressed in mammalian tissues and it has a well-recognized function in the initial phase of peroxisomal fission when it remodels and elongates peroxisomal membranes (Delille et al., 2010; Yoshida et al., 2015; Schrader et al., 2016). The functions of PEX11 α and PEX11 γ are less clear (Schrader et al., 2016). Of the PEX11 proteins in mammals, only PEX11 β deficiency was associated with the pathology of peroxisome biogenesis disorders (PBDs) (Li and Gould, 2002; Thoms and Gartner, 2012; Schrader et al., 2016).

In trypanosomes, three PEX11 family proteins are known, namely, PEX11, GIM5A and GIM5B (Lorenz et al., 1998; Maier et al., 2001; Voncken et al., 2003). Like in mammals, yeast, and plants, both N- and C-termini of *Tb*PEX11 are exposed to the cytosol (Lorenz et al., 1998). Overexpression of *Tb*PEX11 induces growth inhibition and transforms the globular glycosomes into long tubule clusters that occupy a large portion of the cytoplasm (Lorenz et al., 1998). Accordingly, *Tb*PEX11 appears to play a role in the proliferation of glycosomes in trypanosomes like its homologs in yeast and mammalian cells (van Roermund et al., 2000) (Reviewed in (Moyersoen et al., 2004)). PEX11 and both GIM5 proteins are essential for the survival of parasites (Lorenz et al., 1998; Voncken et al., 2003). At primary sequence level, PEX11 family proteins contain several conserved helices particularly in the N-terminal region (Lorenz et al., 1998; Opalinski et al., 2018). PEX19 binding sites have been identified in various glycosomal membrane proteins (Saveria et al., 2007), but not in *Tb*PEX11. Therefore, in this study, we characterized PEX19 binding sites of PEX11 from *Trypanosoma brucei* and *Saccharomyces cerevisiae*. *Tb*PEX11 contains two PEX19 binding sites, the N-terminal PEX19 binding site (BS1) in PEX11 is highly conserved across different organisms and is required for maintenance of the steady-state concentration as well as efficient targeting to peroxisomes and glycosomes in both baker's yeast and *T. brucei*. Deletion or mutations of the

TABLE 1 Strains and plasmids.

Sl no.	Expression in	Construct	Primer pair	Restriction sites	Cloned in vector
1	<i>E. coli</i>	GST- <i>Tb</i> PEX19	RE2926 - RE7038	BamHI/XhoI	pGEX4T-2
2	<i>E. coli</i>	GST- <i>Hs</i> PEX19	pAH5 Halbach et al. (2005)		
3	<i>S. cerevisiae</i>	GAL4 AD- <i>Sc</i> PEX14	Albertini et al. (1997)		
4	<i>S. cerevisiae</i>	GAL4 BD- <i>Sc</i> PEX17 _{167-199aa}	Girzalsky et al. (2006)		
5	<i>S. cerevisiae</i>	GAL4 AD- <i>Tb</i> PEX19 _{1-285aa}	RE3310 - RE3311 (pIA13, AG Erdmann)	SalI/NotI	pPC86
6	<i>S. cerevisiae</i>	GAL4 BD- <i>Tb</i> PEX11 _{1-218aa}	RE7303 - RE7306	SalI/NotI	pPC97
7	<i>S. cerevisiae</i>	GAL4 BD- <i>Tb</i> PEX11 _{1-89aa}	RE7303 - RE7305	SalI/NotI	pPC97
8	<i>S. cerevisiae</i>	GAL4 BD- <i>Tb</i> PEX11 _{90-218aa}	RE7304 - RE7306	SalI/NotI	pPC97
9	<i>S. cerevisiae</i>	GAL4 BD- <i>Tb</i> PEX11 _{1-76aa}	RE8882—RE8883	Quick change PCR	pPC97
10	<i>S. cerevisiae</i>	GAL4 BD- <i>Tb</i> PEX11 _{1-89aa} (S 25 D)	RE7713 - RE7714	Quick change PCR	pPC97
11	<i>S. cerevisiae</i>	GAL4 BD- <i>Tb</i> PEX11 _{1-89aa} (S 25 P)	RE7715 - RE7716	Quick change PCR	pPC97
12	<i>S. cerevisiae</i>	GAL4 BD- <i>Tb</i> PEX11 _{1-89aa} (L 31 P)	RE7717 - RE7718	Quick change PCR	pPC97
13	<i>S. cerevisiae</i>	GAL4 BD- <i>Tb</i> PEX11 _{1-89aa} (S 25 P, L 31 P)	RE7715 - RE7716, RE7717 - RE7718	Quick change PCR	pPC97
14	<i>S. cerevisiae</i>	GAL4 AD- <i>Hs</i> PEX19	RE7706 - RE7707	SalI/NotI	pPC86
15	<i>S. cerevisiae</i>	GAL4 BD- <i>Hs</i> PEX11 _{1-73aa}	RE7843 - RE7844	SalI/NotI	pPC97
16	<i>S. cerevisiae</i>	GAL4 BD- <i>Hs</i> PEX11 _{1-73aa}	RE7708 - RE7709	SalI/NotI	pPC97
17	<i>S. cerevisiae</i>	GAL4 BD- <i>Hs</i> PEX11 _{1-74aa}	RE7845 - RE7846	SalI/NotI	pPC97
18	<i>S. cerevisiae</i>	<i>Sc</i> PEX11-GFP	Boutouja et al. (2019)		
19	<i>S. cerevisiae</i>	<i>Sc</i> PEX11 (L 35 P)-GFP	RE8063 - RE8064	Quick change PCR	pUG35
20	<i>T. brucei</i>	<i>Tb</i> PEX11-GFP	RE8070 - RE8071	BstBI/BamHI	pGN1
21	<i>T. brucei</i>	<i>Tb</i> PEX11 _{Δ13-35aa} -GFP	RE8072 - RE8073	Quick change PCR	pGN1
22	<i>T. brucei</i>	<i>Tb</i> PEX11 _{Δ77-99aa} -GFP	RE8074 - RE8075	Quick change PCR	pGN1
23	<i>T. brucei</i>	<i>Tb</i> PEX11 _{1-90aa} -GFP	RE7378 - RE7379	ApaI/BamHI	pGN1
24	<i>T. brucei</i>	<i>Tb</i> PEX11 _{1-90aa-Δ13-35aa} -GFP	RE8072 - RE8073	Quick change PCR	pGN1
25	<i>T. brucei</i>	<i>Tb</i> PEX11 _{1-90aa-Δ2-11aa} -GFP	RE8096 - RE7379	BstBI/BamHI	pGN1

PEX19 binding site in *Tb*PEX11 (second PEX19 BS, i.e., BS2) or *Sc*PEX11 (single PEX19 BS) results in a mislocalization of the proteins to mitochondria. Trypanosomes contain multiple small glycosomes, but harbor a single mitochondrion ([Tyler et al., 2001](#)). We show that the extreme N-terminal region of *Tb*PEX11 contains a cryptic N-terminal signal that directs PEX11 to the mitochondrion if its glycosomal transport is blocked.

2 Materials and methods

2.1 Cloning

Escherichia coli, yeast, and *Trypanosoma* expression plasmid constructs and cloning strategies are listed in [Table 1](#), and oligonucleotide sequences are listed in [Table 2](#). Point mutations in *Sc*PEX11, *Tb*PEX11_{1-89aa}, and the gene fragment deletions

(*Tb*PEX11_{1-76aa} and *Tb*PEX11-GFP constructs) were generated by overlap extension PCR. Sequences of the constructs, mutations, and gene fragment deletions were verified for all constructs by automated Sanger sequencing.

2.2 Cell culture

2.2.1 *Trypanosoma*

Trypanosoma procyclic form (PCF) 29–13 cell line (co-expressing T7 RNAP and TetR) was used in this study. PCF cells were grown in SDM-79 medium supplemented with 10% FBS at 28°C ([Brun and Schonenberger, 1979](#); [Krishna et al., 2023](#)). PCF cultures were maintained at 1×10^6 – 30×10^6 cells/mL. Transfections were performed with NotI-linearized plasmid constructs (pGN1-*Tb*PEX11 constructs), which was genomically integrated into the rRNA locus in the genome of cell line 29–13. Clones were selected using Blasticidin (10 µg/mL) as described previously ([Kalel et al., 2015](#)).

2.2.2 Yeast

S. cerevisiae wild-type strain BY4742 (for microscopy) and strain PCY2 (WT or Δ pex19 for yeast two-hybrid assay) were grown in double dropout SD synthetic media as described in section 2.3 and 2.4.2. Yeast cells were transformed by the traditional Lithium-acetate method (Gietz and Woods, 2002).

2.2.3 Escherichia coli

Escherichia coli strain TOP10 was used for all plasmid amplifications and BL21 (DE3) strain was used for heterologous expression of recombinant GST-PEX19 fusion proteins. Liquid *E. coli* cultures were grown at 37°C under continuous shaking in LB medium containing the appropriate selective antibiotic (100 µg/mL Ampicillin).

2.3 Yeast two-hybrid analysis (Y2H)

Y2H studies were performed based on the Yeast protocols handbook (Clontech, Protocol No. PT3024-1, Version No. PR742227). Full length or various truncations of *Trypanosoma* or Human PEX11 were cloned in pPC97 vector containing GAL4-DNA Binding Domain (BD) and full-length *Trypanosoma* or human PEX19 were cloned in pPC86 vector containing GAL4-Activation domain (AD), as described in Table 1. Co-transformation of various two-hybrid plasmids i.e., BD and AD constructs were performed in WT PCY2 or Δ pex19 PCY2 strain in case of HsPEX19-HsPEX11 constructs. The clones were selected on SD synthetic medium without tryptophan and leucine. A filter-based β -galactosidase assay and liquid culture assay using ONPG were performed in three replicates as described in the Yeast protocols handbook (Clontech).

2.4 Microscopy

2.4.1 Trypanosoma

Trypanosoma stable cell lines (Procylic 29:13) encoding various tetracycline inducible PEX11-GFP constructs (full-length and mutants) were induced with 1 µg/mL tetracycline or treated with DMSO alone as negative control. Cells were sedimented and fixed by resuspension in 4% paraformaldehyde in PBS (phosphate-buffered saline, pH 7.4) at 4°C for 15 min. Fixed *Trypanosoma* cells were washed two times with PBS and stored at 4°C in a dark box. For imaging, fixed cells were immobilized on a glass slide (StarFrost 76 × 26 mm, Knittel Glass) pre-coated with 10% (v/v) of poly-L-lysine (Sigma-Aldrich) in water for 1 h at room temperature (RT). Further, the cell membranes were permeabilized with PBS containing 0.125% Triton X-100 and incubated for 10–15 min, followed by blocking with PBS containing 3% BSA, 0.25% Tween-20 for 1 h at RT. Rabbit α -Aldolase antibody (1:500 in blocking buffer) was used as glycosomal marker and incubated at RT for 1 h. Following 5 washes with PBS, anti-rabbit Alexa fluor 594 secondary antibodies (1:200 dilution) in PBS was applied and incubated for 30 min at RT in the dark. Further, the stained samples were washed, dried, and layered with anti-fading

mounting medium, i.e., Mowiol with DAPI (4',6-diamidino-2-phenylindole).

For mitochondrial staining, tetracycline-induced or uninduced (DMSO-treated) *Trypanosoma* cells were harvested and resuspended in the culture medium containing 75 nM MitoTracker® Deep Red and incubated for 5 min at 28°C. Following incubation, cells were washed with PBS twice and resuspended in the culture medium and further incubated for 30 min at 28°C. Subsequently, cells were fixed with 4% paraformaldehyde in PBS, and samples were prepared for microscopy as mentioned above.

Glycosome- or mitochondrion-stained cells were visualized and imaged with a Zeiss Elyra microscope and were analyzed using Zeiss Zen 3.2 software (blue edition). Both aldolase and MitoTracker which are markers for glycosome and mitochondrion respectively, are pseudo-colored to magenta for visualization.

2.4.2 Yeast

BY4742 yeast strain co-transformed with the plasmids encoding ScPEX11-GFP (WT (Boutouja et al., 2019) and L₃₅ to P mutant, with the endogenous promoter) and DsRed-SKL (as a peroxisomal reporter (Kuravi et al., 2006)) were grown overnight (16 h) with shaking in an SD synthetic medium without uracil and histidine. Next day the precultures were diluted to 0.1 OD₆₀₀/mL and were incubated under shaking until the cell density reached 0.6–0.8 OD₆₀₀/mL. After incubation, 1–2 mL cultures were harvested and washed with water. For mitochondrial staining, 5 mL of yeast cells, grown to a density of 0.6–0.8 OD₆₀₀/mL, expressing the ScPEX11 constructs were stained with 150 nM MitoTracker™ Orange CMTMros (Invitrogen) for 30 min with shaking in dark. Following incubation, 1–2 mL cultures were harvested and washed with water. All incubation steps were performed at 30°C. Yeast cells expressing various fluorescent proteins were directly visualized microscopically without fixation. Microscopy was performed with Carl Zeiss Microscope, using the Axiovision 4.6.3 software, and images were analyzed using Zen 3.2 (blue edition), a Carl Zeiss software. The DsRed-SKL, a peroxisomal reporter is pseudo-colored to magenta for visualization.

2.5 Peptide array

The immobilized peptides of 15-amino acids length, sequentially overlapping by 13 residues (2aa shift), representing the entire sequence of TbPEX11 or the N-terminal domains of three human PEX11 isoforms were synthesized on a cellulose membrane as described previously (Hilpert et al., 2007; Neuhaus et al., 2014). The peptide array was first washed with ethanol for 10 min with gentle shaking followed by three washes with TBS (50 mM Tris, 137 mM NaCl, 2.7 mM KCl, adjusted to pH 8) for 10 min each. Further, the peptide array was incubated with a blocking buffer (TBS +3% BSA +0.05% Tween-20) for 2 h at room temperature (RT). The purified recombinant proteins GST-TbPEX19, GST-HsPEX19, or GST alone (10 mL of 1 µM solution prepared in blocking buffer) were incubated with the arrays for 1 h at 4°C. Then, the arrays were washed three times for 10 min at RT with TBS, and

TABLE 2 Oligonucleotides.

Primer	Sequence 5' to 3'
RE2926	GATCGGATCCATGTCTCATCCCGACAATGAC
RE3310	GATCGTCGACGATGTCTCATCCCGACAATGAC
RE3311	GATCGCGGCCGCTACACTGATGGTTGCACATCG
RE7038	CCGCTCGAGTTACACTGATGGTTGCACATCGGCAAGTCC
RE7303	TGGACCGTCGACGATGTCTGAGTTCCAAAGGTTTGT
RE7304	AATATAGTCGACTAAGTTCCTCCGCGTGTGTGC
RE7305	AAGATAGCGGCCGCTTACAAGACCTCTTTCATGTTGAC
RE7306	AATAAGCGGCCGCTATTTGATCTTGTCCAGTTCAA
RE7378	AAGATAGGGCCCATGTCTGAGTTCCAAAGGTTTGT
RE7379	AAATGGATCCGATCCGCTTCCCTTCAAGACCTCTTTCATGTTGAC
RE7706	AAGACGTCGACCATGGCCGCGCTGAGGAAGGCTG
RE7707	AAGACGCGGCCGCTCACATGATCAGACACTGTTCA
RE7708	AAGATGTCGACAATGGACGCTGGGTCCGCTTCAAG
RE7709	AAGACGCGGCCGCTTATCTTTGGCTGACTCAAGG
RE7713	GCCTTAAAGACACCATCAAATGCCTTTAGAATCTTGTGCGGGC
RE7714	GCCGCGACAAGATTCTAAAGGCATTTGATGGTGTCTTTAAGGC
RE7715	CTTAAAGACACCAGGAAATGCCTTTAGAATCTTGTGCGGG
RE7716	CCGCGACAAGATTCTAAAGGCATTTCTGGTGTCTTTAAG
RE7717	GTGTCGAGGGAGCCAGGTGCCTTAAAGACAC
RE7718	GTGTCTTTAAGGCACCTGGCTCCCTCGACAC
RE7843	AGAAGTCGACAATGGACGCCTTACCCGCTTACC
RE7844	AAGAGCGGCCGCTTACTGCTCAGTTGCCTGTATAG
RE7845	AAGAAGTCGACAATGGCGTCGCTGAGCGCCCTGG
RE7846	AAGAGCGGCCGCTTATTGCTTAGTGTAGACAAAACA
RE8063	CTGCTAAAAATCTTGTGATACTGCAGTAATCTGAGAACCTTTTCTCTGC
RE8064	GCAGAGAAAAGTTCTCAGATTACTGCAGTATCCAGCAAGATTTTAGCAG
RE8070	AAGAATTCGAAATGTCTGAGTTCCAAAGGTTTGT
RE8071	AAGACGGATCCGATTTGATCTTGTTCAGTTCAA
RE8072	TTCTTGAGACCTGTCAGAGCCGCTCAAAG
RE8073	GACAGGTCTCAAGAAGCTTAACAAACCTTGG
RE8074	TTCAGGATTATGTGCTCGGCGACAATG
RE8075	GCACATAATCCTGAATGGCATTCTGC
RE8096	AAGACTTCGAAATGGAGCAGACAGATGGCCGCGAC
RE8882	TTCAGGATTAAGCGGCCGCTAAGTAAG
RE8883	CCGCTTAATCCTGAATGGCATTCTGCATC

subsequently incubated with the anti-GST monoclonal antibody (Sigma, 1:2000) at RT for 1 h. Followed by three washes with TBS (10 min each), a secondary antibody (Horseradish peroxidase-coupled anti-mouse IgGs, 1:5,000 in blocking buffer) was applied,

and the array was further incubated for 1 h at RT. After three washes with TBS, the array was scanned with chemiluminescence substrate (WesternBright Sirius) using Azure sapphire biomolecular imager.

2.6 Protein expression and purification, *in vitro* pull-downs and AlphaScreen binding assay

2.6.1 Protein expression and purification

The expression plasmids pGEX4T2, pGEX4T2-*Tb*PEX19 or pGEX4T1-*Hs*PEX19, encoding for GST, GST-*Tb*PEX19 or GST-*Hs*PEX19, respectively, were transformed into BL21 (DE3) *E. coli* strain. Single colonies were inoculated in LB medium containing ampicillin and incubated overnight with shaking at 37°C. On the following day, the cultures were reinoculated with 0.1 OD₆₀₀/mL and further incubated at 37°C with shaking, until the cell density reached 0.6 OD₆₀₀/mL. Protein expression was induced with 1 mM IPTG for 4 h at 30°C. Harvested cell pellets were stored at -20°C before use. For protein purification, *E. coli* cell pellets were resuspended in PBS with protease inhibitors (5 µg/mL Antipain, 2 µg/mL Aprotinin, 0.35 µg/mL Bestatin, 6 µg/mL Chymostatin, 2.5 µg/mL Leupeptin, 1 µg/mL Pepstatin, 0.1 mM PMSF, 25 µg/mL DNase and 1 mM DTT). Cells were disrupted using EmulsiFlex and unbroken cells were removed by centrifugation at 4,500 rpm for 15 min (rotor SX4400, Beckman Coulter). The resulting supernatant (SN1) was subjected to a high-speed centrifugation at 14,000 rpm for 1 h (rotor SS-34, Thermo Scientific), which yielded supernatant 2 (SN2), a soluble fraction that included overexpressed proteins. Proteins were purified by affinity chromatography using Glutathione Agarose 4B beads (Macherey-Nagel). To this end, SN2 was incubated with the pre-equilibrated glutathione agarose beads for 2 h in a tube rotator. After collection of the flow-through, using a gravity flow column, the protein-bound beads were washed five times with PBS. Proteins were eluted with 10 mM reduced glutathione in 50 mM Tris-Cl (pH 8). The buffer of the eluted protein was exchanged to PBS using Amicon centrifugation tubes with molecular weight cut-off (MWCO) 10 kDa. The concentration of the proteins was determined by the Bradford method (Thermo, Coomassie Plus assay kit), and protein aliquots were stored at -80°C. All the purification steps were performed at 4°C.

2.6.2 *In vitro* pull-down

20 µL bed volume Glutathione Agarose 4B beads (Macherey-Nagel) were incubated with 200 µg of recombinantly purified GST and GST-*Tb*PEX19 proteins in separate tubes for 2 h at 4°C with gentle rotation. Following incubation, beads were washed with PBS to remove unbound proteins. Subsequently, 25 µg of C-terminally His₆-tagged synthetic peptides of crude grade, containing the corresponding *Tb*PEX19 binding regions in *Tb*PEX11 (BS1-BS3) were loaded to the respective tubes and were incubated for 2 h at 4°C with gentle rotation to allow binding of the peptides to GST-*Tb*PEX19 or control GST. Following washes with PBS, the bound proteins/peptides were eluted with 50 µL 10 mM reduced glutathione in 50 mM Tris (pH 8). The eluted samples were analyzed by SDS-PAGE followed by Coomassie staining and immunoblotting. The sequences of the *Tb*PEX11 peptides used for the pull-down are as follows, BS1: QTDGRDKILKAFSGVFKALGSLD-GS-His₆, BS2: CRAKGKVNMEKVLKFLRVLCNLF-GS-His₆ and BS3: VLDVVVALYGALQKRASDPATS-GS-His₆.

2.6.3 AlphaScreen binding assay

N-terminal GST tagged *Tb*PEX19 and *Tb*PEX11 peptides with C-/N-terminal His₆ were used for the interaction study with the

AlphaScreen system. The final reaction volume used for the study was 25 µL, which consist of 5 µL of each protein solution (30 nM for PEX19 and 300 nM of PEX11 peptides), 5 µL of buffer, and 5 µL of solution for each of the donor and acceptor beads (5 µg/mL). The above solutions were prepared in reaction buffer [0.5% BSA v/v, PBS (pH7.4)] on the day of the assay. Compounds were incubated with the proteins for 30 min at room temperature (RT). 5 µL of AlphaScreen Nickel-chelate acceptor beads (cat. no. 6760619C, PerkinElmer[®]) were added to the above mixture following 15 min incubation at RT. 5 µL AlphaScreen Glutathione donor beads (cat. no. 6765300, PerkinElmer[®]) were added to the mixture. The complete 25 µL reaction solutions were incubated for 45 min at RT in the dark, and Alpha signals were captured with Cytation 5 plate reader (BioTek[®]) with the gain value set at 180. All above concentrations mentioned for the AlphaScreen assays were final concentrations unless otherwise stated. The sequences of the *Tb*PEX11 peptides used for the AlphaScreen assay are as follows, BS1: QTDGRDKILKAFSGVFKALGSLD-GS-His₆, His₆-GS-QTDGRDKI LKAFSGVFKALGSLD and BS2: CRAKGKVNMEKVLKFLRV LCNLF-GS-His₆. The binding assay were performed in three biological replicates, with 3 technical replicates each.

2.7 Immunoblotting

Proteins separated by SDS-PAGE were transferred on a nitrocellulose membrane with a pore size of 0.45 µm (Amersham Biosciences). Blotting was performed by using the MiniProtein III cell (BioRad) with blot transfer buffer (Dunn carbonate buffer) for 1 h with a constant current of 300 mA per chamber. Further, the membrane was blocked for 1 h at room temperature (RT), under constant swirling with 3% BSA in blot washing buffer (TBS with 0.05% Tween-20) to avoid nonspecific binding of antibodies. Then, the membrane was washed three times for 5 min at RT, and subsequently incubated with the primary antibodies in blot washing buffer at 4°C overnight. Following primary antibodies were used in this study: mouse anti-GFP (Sigma, 1:2,000), anti-GAL4 AD/-BD (Santa Cruz Biotechnology, 1:1,000) or anti-His₆ (Invitrogen, 1:2,000); rabbit anti-*Trypanosoma* Aldolase (1:20,000) or Enolase (1:20,000), and anti-Porin (*S. cerevisiae*, 1:10,000). After three washing steps, the corresponding secondary antibodies i.e., goat anti-rabbit IRDye 680 or goat anti-mouse IRDye 800CW (LI-COR Biosciences, both 1:15,000 in blot wash buffer) were applied, and the membrane was further incubated for 30 min at RT in the dark. Following three washes, immunoblots were scanned using the Li-Cor Odyssey 9120 Infrared Imaging System.

2.8 Statistical analysis

Microscopic data was collected from two independent *S. cerevisiae* or *T. brucei* cultures. Images were quantified using Pearson's correlation coefficient, which was calculated with colocalization tool of Zen 3.6 pro (blue edition). Statistical significances for colocalization studies were calculated using a one-way ANOVA (mixed) by Dunnett's multiple comparisons test (comparison with WT control) with each row representing matched or repeated measures. Statistical analysis for AlphaScreen

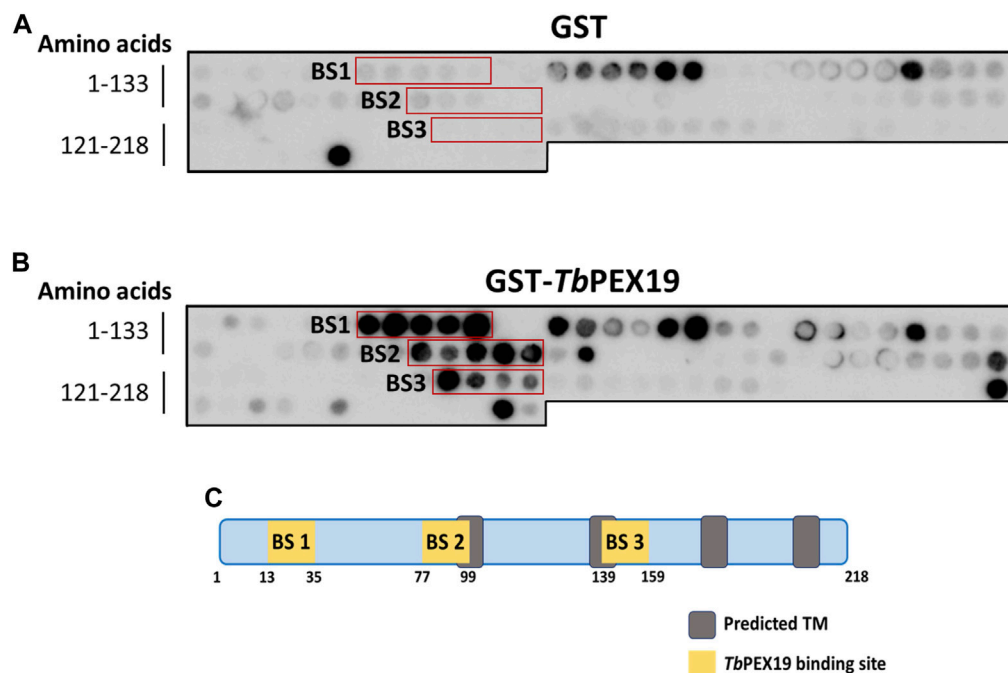


FIGURE 1

Identification of PEX19 binding sites in *Trypanosoma* PEX11 using synthetic peptide arrays. Synthetic 15-mer peptides with 2-amino acids shifts corresponding to the complete *Tb*PEX11 protein sequence were synthesized on cellulose membrane and probed with GST as negative control (A) or GST-*Tb*PEX19 (B). Bound analyte was immuno-detected using primary antibodies against GST and horseradish peroxidase coupled secondary antibodies, followed by the signal detection using chemiluminescence. Three regions in *Tb*PEX11 showed clear and specific interaction with *Tb*PEX19 as compared to the GST control (red boxes, marked BS1-BS3). (C) Scheme of *Tb*PEX11 showing the identified binding regions in relation to transmembrane segments predicted using Phobius webtool (<https://phobius.sbc.su.se/>) (Supplementary Figure S2).

results was done using two-way ANOVA with Bonferroni's multiple comparison test (comparison with respective controls) with the values obtained from three independent biological replicates, each with three technical replicates.

3 Results

3.1 Identification and validation of PEX19 binding sites in *Trypanosoma brucei* PEX11

PEX19 acts as a cytosolic chaperone and receptor for the import of newly synthesized class I peroxisomal membrane proteins (PMPs), except the class II PMP i.e., PEX3, which can be imported independent of PEX19 (Sacksteder et al., 2000; Jones et al., 2004). PMPs contain multiple PEX19 binding sites, which are well characterized in yeast and humans. This includes the most abundant yeast PMP Pex11p and related PEX11-family proteins Pex25p and Pex27p (Rottensteiner et al., 2004; Halbach et al., 2005). In trypanosomatid parasites, PEX19 binding sites have been identified in various glycosomal membrane proteins as well as parasite specific PEX11 family proteins GIM5A/B (Saveria et al., 2007). However, the PEX19-binding sites (-BS) in parasite PEX11 remained uncharacterized. To identify these binding sites, we obtained synthetic peptide arrays, containing consecutive 15-amino acid peptides with two amino acid shifts, representing the

entire sequence of *Tb*PEX11. Affinity purified recombinant GST-*Tb*PEX19 (Purification profile described in Supplementary Figure S1), or GST alone were incubated with the arrays and bound proteins were immuno-detected using monoclonal anti-GST antibodies. Immunodetection of at least three consecutive spots were considered as potential PEX19 binding sites (Rottensteiner et al., 2004). Comparison of control and test peptide arrays revealed the presence of three potential PEX19 binding sites (BS1-BS3) in *Tb*PEX11 (Figure 1). The topological prediction of transmembrane domains (TMDs) using Phobius webserver (Kall et al., 2007) indicates that *Tb*PEX11 contains four TMDs and an N-terminal extension of about 90 amino acids to the cytosol (Supplementary Figure S2). The first PEX19 binding site (BS1) is present close to the N-terminus of *Tb*PEX11 between amino acid (aa) residues 13–35, the second and third PEX19 binding sites are located between aa77–99 and aa139–159, respectively, in proximity of the first and second predicted transmembrane domains (Figure 1C). Both N- and C-termini of *Tb*PEX11 face the cytosol (Lorenz et al., 1998), which implies that the BS1 would remain exposed to the cytosol even after targeting and insertion of *Tb*PEX11 into the glycosomal membrane.

PEX19 binding motifs are conserved between peroxisomal proteins of yeast or mammals and trypanosomal glycosomal proteins (Saveria et al., 2007). Probing of the *Tb*PEX11 peptide array with GST-tagged recombinant human PEX19 also revealed a similar binding pattern (Supplementary Figure S3) as observed with *Tb*PEX19 (Figure 1). This further demonstrates the conservation of

and strong interaction with the full length *Tb*PEX19, in both plate-based (sensitive) and liquid Y2H assays (quantitative) (Figure 2A). Construct that lacks the N-terminal domain but contains BS3 (*Tb*PEX11_{90-218aa}) did not interact with *Tb*PEX19. *Tb*PEX11₁₋₈₉ contains BS1 as well as partial BS2. We also tested a shorter construct that contains only BS1 (*Tb*PEX11₁₋₇₆), which still showed a strong interaction with *Tb*PEX19. Immunoblotting confirmed that all constructs are expressed in yeast at correct molecular weights (Figure 2B). Furthermore, we opted to introduce two mutations in *Trypanosoma* PEX11. The first mutation replaced serine 25, which is in the *Tb*PEX19 BS1 region, by aspartate to mimic phosphorylation (based on the post-translational modifications database). For the second mutation, we referred to a study in baker's yeast, which showed that replacing leucine at position 35 by proline results in the loss of interaction (Rottensteiner et al., 2004). We aligned the sequence with ScPEX11 and chose the closest leucine residue (position 31) for replacement by proline. Mutation of serine₂₅ to aspartate i.e., phospho-mimicking did not affect the interaction, whereas mutation of serine₂₅ or leucine₃₁ individually and together to proline within BS1 in *Tb*PEX11₁₋₈₉ led to a reduced or complete abolishment of the interaction with *Tb*PEX19 (Supplementary Figure S4). Based on the peptide blot and the Y2H studies, it can be concluded that BS1 is a *bona fide* PEX19 binding motif.

As an alternative, we obtained C-terminally His₆-tagged synthetic peptides of *Tb*PEX11 corresponding to the three putative PEX19 binding sites. Affinity pull-down was performed with GST-*Tb*PEX19 or GST alone as negative control, which were bound to the glutathione affinity beads. Glutathione eluates of the *in vitro* pull-downs were analyzed by Coomassie staining as well as immunoblotting using anti-His₆ tag antibodies (Figure 2C; full profile of the pull-downs is shown in Supplementary Figure S5). The analysis shows that the synthetic peptide corresponding to BS2 (running at ~10 kDa) is efficiently retained with *Tb*PEX19 but not with GST alone. Similar binding of the BS2 representing peptide of *Tb*PEX11 was also observed with recombinant human GST-PEX19 (not shown). The synthetic peptides corresponding to BS1 and BS3 (both running at ~10 kDa) did not bind to recombinant GST-*Tb*PEX19 in this assay. The third putative PEX19 binding site (BS3) in *Tb*PEX11 that was identified in the peptide array analysis (Figure 1) could not be further validated by the methods employed here and was not considered further.

Finally, we analyzed the interaction of BS1 and BS2 with *Tb*PEX19 with the more sensitive AlphaScreen assay. This assay was performed using C-terminally His₆-tagged peptides that represent the *Tb*PEX11 binding sites with GST-*Tb*PEX19 or GST as negative control (Supplementary Figure S6). Again, the BS2 showed a clear interaction with *Tb*PEX19, while the BS1 did not interact. As the interacting BS1 containing region was N-terminally tagged in the Y2H assay (Figure 2A), we considered that the orientation of the tag might have an influence and therefore analyzed the interaction of an N-terminally tagged BS1-peptide, which indeed showed a significant interaction with *Tb*PEX19 (Supplementary Figure S6). Taken together this study identified two PEX19 binding sites in *Tb*PEX11 (BS1 and BS2).

3.2 Role of PEX19 binding sites in glycosomal targeting of *Tb*PEX11

We performed immunofluorescence microscopy analysis to assess the relevance of the newly identified PEX19 binding sites for the topogenesis of *Tb*PEX11. Tetracycline inducible stable cell lines of *Trypanosoma* were generated, which express C-terminally GFP-tagged full-length *Tb*PEX11 and variants lacking either BS1 or BS2. Glycosomal localization of the constructs was investigated by analysis of colocalization of the fluorescent GFP-fusions of *Tb*PEX11 with the glycosomal marker enzyme aldolase, which was monitored by immunofluorescence microscopy. Overexpressed *Tb*PEX11_{WT}-GFP colocalized with the glycosomal marker, indicative for its glycosomal localization (Figure 3A, upper panel). However, frequently glycosomes appeared to cluster, confirming an earlier study reporting that overexpression of *Tb*PEX11 results in clustering of glycosomes in bloodstream form of *T. brucei* (Lorenz et al., 1998). The GFP fluorescence of cells expressing both truncated *Tb*PEX11 variants was much weaker in comparison to the wild-type protein and clustering of glycosomes was not seen. This is explained by the decreased steady-state concentration of both truncated proteins, which is much lower in comparison to the full-length *Tb*PEX11 as indicated by the corresponding immunoblots. (Figure 3D). However, the fluorescence was bright enough to allow investigation of their subcellular localization. *Tb*PEX11 lacking BS1 (*Tb*PEX11_{ΔBS1}-GFP) still showed a partial glycosomal localization (Figure 3A, Middle panel), while the *Tb*PEX11 variant lacking BS2 (*Tb*PEX11_{ΔBS2}-GFP) was mislocalized, as indicated by the lacking colocalization with the glycosomal marker (Figure 3A, lower panel). Taken together this result demonstrated that deficiency in either BS1 or BS2 affects the steady-state concentration of *Tb*PEX11. Thus, binding of PEX19 to either of these sites might stabilize the protein. This is in agreement with studies in yeast, which showed that various PMPs, including PEX11, are unstable and their steady state levels are significantly reduced in PEX19- or PEX3-deficient cells (Hettema et al., 2000). In the absence of BS1, the remaining small amount of *Tb*PEX11 is still directed to glycosomes, while in the absence of BS2, PEX11 is mistargeted, indicating that BS2 is essential for glycosomal targeting of *Tb*PEX11.

In yeast, PEX11 mislocalizes to mitochondria in cells lacking peroxisomal membranes (Hettema et al., 2000; Mattiazzi Usaj et al., 2015). To assess whether mislocalized *Tb*PEX11 is targeted to mitochondria also in trypanosomes, mitochondrial staining was performed. Indeed, colocalization of the truncated *Tb*PEX11 with the MitoTracker indicated that *Tb*PEX11 lacking BS2 is mistargeted to the mitochondrion (Figure 3B, lower panel).

Multiple sequence alignment of the N-terminal region comprising BS1 of *Trypanosoma*, yeast, human, and plant PEX11 family proteins or isoforms indicates a high degree of sequence conservation, suggesting that the region corresponding to trypanosomal BS1 is conserved among PEX11 species (Figure 4A). To investigate the capacity of this region of human PEX11 proteins for PEX19 binding, we obtained synthetic peptide array of N-terminal soluble domains of all three human PEX11 isoforms (15mer peptides with 2-amino acids shifts). The arrays were probed with GST alone as a negative control, which showed little or no background (Figure 4B, upper panel). Probing

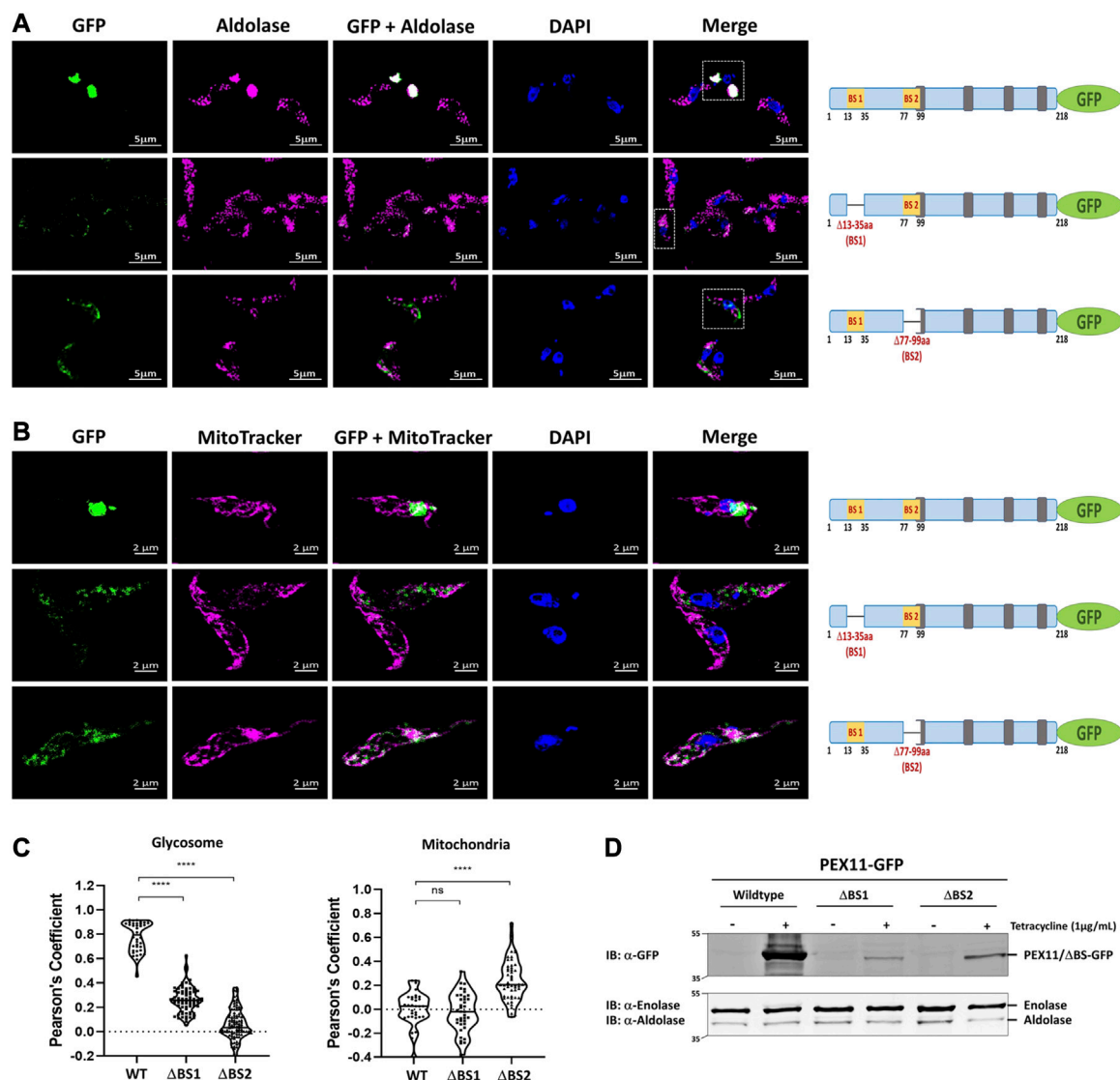


FIGURE 3

PEX19 binding sites are required for maintenance and essential for glycosomal targeting of *Tb*PEX11. **(A)** Binding site 2 (BS2) is required for glycosomal targeting of *Tb*PEX11. *Trypanosoma brucei* parasites (procyclic form) expressing tetracycline-induced and C-terminally GFP tagged *Tb*PEX11 constructs (wildtype or mutant proteins lacking PEX19 binding sites) were analyzed for localization of the GFP fusion proteins, the glycosomal marker aldolase, as well as the DAPI-stained nucleus and kinetoplast by fluorescence- or immunofluorescence microscopy. The GFP fusion of wildtype *Tb*PEX11 (upper panel) did colocalize with the glycosome marker aldolase (pseudo-colored to magenta). It is also evident that the overexpression of the full-length *Tb*PEX11 results in the clustering of glycosomes as previously reported (Lorenz et al., 1998). The mutant lacking the first PEX19 binding site (middle panel) partially colocalized with the glycosome marker aldolase. In this case, a clustering of glycosomes was not seen, most likely as the steady-state concentration of the truncated protein was much lower than the corresponding full-length *Tb*PEX11 (see below). PEX11-GFP harboring deletion of BS2 ($\Delta 77-99$ aa) did not colocalize with the glycosomal marker aldolase (lower panel), but instead showed mislocalization to mitochondrion as demonstrated by colocalization with the mitochondrial marker MitoTracker (pseudo-colored to magenta) **(B)**. Scale bar—5 μ m and \sim 2 μ m. Schematic representation of the various PEX11-GFP constructs is shown on the right. **(C)** Quantification of the colocalization to glycosomes (left) or mitochondrion (right). The Pearson's coefficient of colocalization to respective organelle is shown. Dots within the violin plot indicates individual Pearson correlation coefficient data points and the central line represents the median. Statistical significance were calculated by one-way ANOVA, with Dunnett's multiple comparisons test ($n \geq 35$ cells). ****, $p < 0.0001$; ns, not significant. **(D)** Analysis of the expression levels of PEX11-GFP (wildtype and mutants) upon tetracycline induction (+/-) by immunoblotting with anti-GFP antibodies. Cytosolic marker enolase and glycosomal marker aldolase served as the loading controls (lower panel). Wildtype *Tb*PEX11 expression was highly induced, resulting in a high steady-state concentration, while the steady-state concentration of both truncation mutants of *Tb*PEX11 were very low in comparison to the wildtype *Tb*PEX11, most likely due to an instability of the *Tb*PEX11 constructs lacking either of the PEX19 binding sites.

the array with GST-*Hs*PEX19 revealed that the peptides from PEX11 γ did not bind PEX19, while PEX11 α and PEX11 β do contain potential PEX19-BS (Figure 4B, lower panel). To validate the interactions, Y2H analysis was performed to investigate the interaction of N-terminal

domains of PEX11 isoforms and human PEX19 (Figure 4C). An interaction was seen only with PEX11 β , in both the plate-based and the liquid assay. Immunoblot analysis of lysates of yeast cell used in Y2H shows that PEX11 α and β were expressed, but not PEX11 γ (Figure 4D).

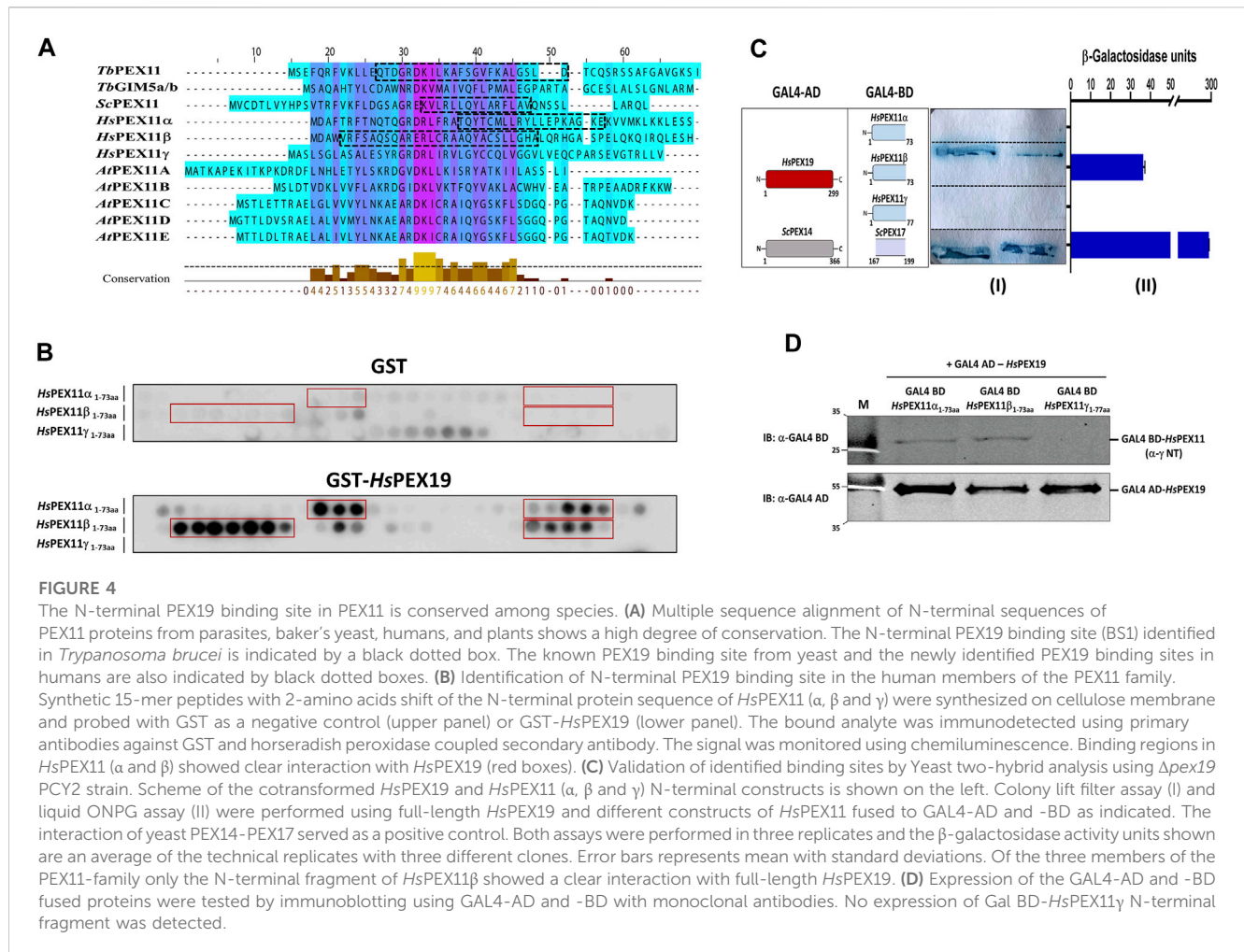


FIGURE 4

The N-terminal PEX19 binding site in PEX11 is conserved among species. (A) Multiple sequence alignment of N-terminal sequences of PEX11 proteins from parasites, baker's yeast, humans, and plants shows a high degree of conservation. The N-terminal PEX19 binding site (BS1) identified in *Trypanosoma brucei* is indicated by a black dotted box. The known PEX19 binding site from yeast and the newly identified PEX19 binding sites in humans are also indicated by black dotted boxes. (B) Identification of N-terminal PEX19 binding site in the human members of the PEX11 family. Synthetic 15-mer peptides with 2-amino acids shift of the N-terminal protein sequence of HsPEX11 (α, β and γ) were synthesized on cellulose membrane and probed with GST as a negative control (upper panel) or GST-HsPEX19 (lower panel). The bound analyte was immunodetected using primary antibodies against GST and horseradish peroxidase coupled secondary antibody. The signal was monitored using chemiluminescence. Binding regions in HsPEX11 (α and β) showed clear interaction with HsPEX19 (red boxes). (C) Validation of identified binding sites by Yeast two-hybrid analysis using Δ*pex19* PCY2 strain. Scheme of the cotransformed HsPEX19 and HsPEX11 (α, β and γ) N-terminal constructs is shown on the left. Colony lift filter assay (I) and liquid ONPG assay (II) were performed using full-length HsPEX19 and different constructs of HsPEX11 fused to GAL4-AD and -BD as indicated. The interaction of yeast PEX14-PEX17 served as a positive control. Both assays were performed in three replicates and the β-galactosidase activity units shown are an average of the technical replicates with three different clones. Error bars represents mean with standard deviations. Of the three members of the PEX11-family only the N-terminal fragment of HsPEX11β showed a clear interaction with full-length HsPEX19. (D) Expression of the GAL4-AD and -BD fused proteins were tested by immunoblotting using GAL4-AD and -BD with monoclonal antibodies. No expression of Gal BD-HsPEX11γ N-terminal fragment was detected.

As PEX11γ was not expressed, no conclusion can be drawn from the negative result of the two-hybrid study. However, the results are clear in that PEX11β indeed does contain a PEX19 binding site in the region that corresponds to trypanosomal BS1.

In yeast, ScPEX11 contains only one PEX19 binding site, spanning amino acids 27–41 (Rottensteiner et al., 2004), that is homologous to trypanosomal BS1. Mutational analysis of this binding site indicated that the L35P mutation completely abolished interaction with ScPEX19 (Rottensteiner et al., 2004). Here we introduced this mutation into the full-length sequence of PEX11 fused to GFP and analyzed its subcellular localization in comparison to wild-type PEX11 by fluorescence microscopy (Figure 5A). As expected, the full-length PEX11-GFP is targeted to peroxisomes as indicated by its co-localization with the peroxisomal marker DsRed-SKL (Figure 5A, middle panel). The PEX11-GFP fusion harboring the L35P exchange, however, was partly mislocalized to tubular structures (Figure 5A, lower panel). We further performed staining of yeast cells that express PEX11_{L35P}-GFP together with a mitochondrial marker (MitoTracker) (Figure 5B, lower panel), confirming that the L35P mutant is mislocalized to mitochondria. Immunoblot analysis of cells shown in Figure 5A show that GFP-tagged wild-type PEX11 is stable, but the steady-state concentration of L35P mutant protein that cannot bind to PEX19 is very low in comparison (Figure 5D).

The data show that PEX11 from *Trypanosoma* and yeast as well as PEX11β from humans contain a conserved N-terminal region that can bind PEX19. This region, corresponding to BS1 in *Trypanosoma*, is required to maintain the steady-state concentration of PEX11 in all studied species, and at least for yeast, it is shown that it is also required for efficient targeting of PEX11 to peroxisomes.

3.3 Cryptic N-terminal targeting signal of trypanosomal PEX11

In the absence of PEX19, PMPs are mislocalized to the cytosol and rapidly degraded, or mislocalized to other membranes. For example, PEX3 localizes to the endoplasmic reticulum (Hoepfner et al., 2005) but many PMPs, including yeast PEX11 and PEX13, accumulate in mitochondria when peroxisomes are absent in the cell (Nuebel et al., 2021). PEX13 that is mislocalized to mitochondria can recruit functional docking and import peroxin complexes to mitochondria and also some peroxisomal matrix proteins (Nuebel et al., 2021). Peroxins also accumulate in mitochondria of Zellweger patient-derived cells leading to mitochondrial dysfunction (Nuebel et al., 2021). This can be rescued by overexpressing mitochondrial quality

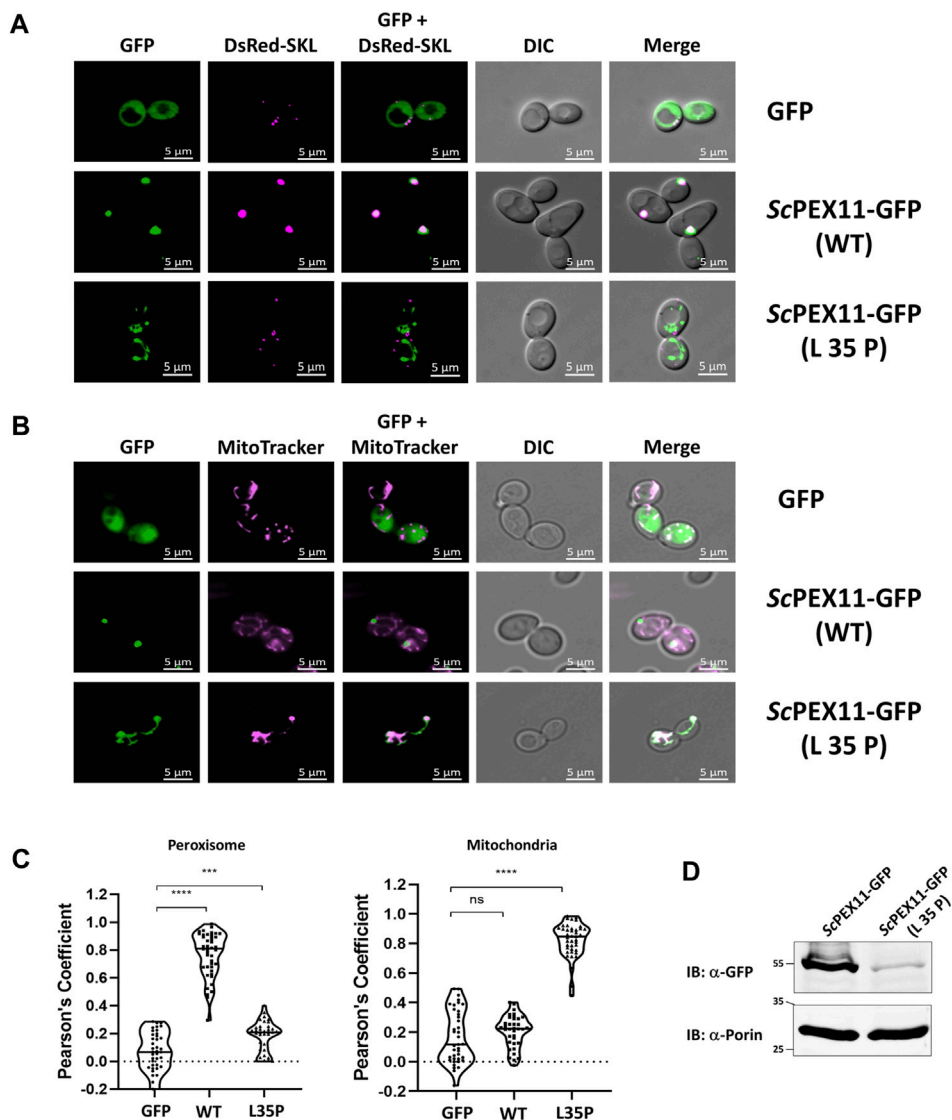


FIGURE 5

The N-terminal binding site for PEX19 is essential for peroxisomal localization of ScPEX11. Plasmids expressing ScPEX11-GFP (wildtype and L35P-mutant) or the peroxisomal marker protein DsRed-SKL were cotransformed in the BY4742 yeast strain. **(A)** Clones expressing GFP fusion proteins and the peroxisomal marker DsRed-SKL were grown on plates and visualized by fluorescence microscopy. Merged images reveal peroxisomal colocalization of ScPEX11-GFP (wildtype) with DsRed-SKL (pseudo-colored to magenta), indicative for its peroxisomal localization. In contrast, the L35P exchange that is known to block PEX19 binding site result in mislocalization of ScPEX11. **(B)** ScPEX11-GFP with mutation L35P mislocalizes to mitochondria as demonstrated by its colocalization with MitoTracker (pseudo-colored to magenta). DIC—Differential Interference Contrast, Scale bar—5 μm. **(C)** Quantification of the colocalization of ScPEX11-GFP to peroxisomes (left) or mitochondria (right). The Pearson's coefficient of colocalization to respective organelle is shown. Dots within the violin plot indicates individual Pearson correlation coefficient data points and the central line represents the median. Statistical significances were calculated by one-way ANOVA, with Dunnett's multiple comparisons test ($n \geq 35$ cells). ****, $p < 0.0001$; ***, $p = 0.0003$; ns, not significant. **(D)** Expression of ScPEX11-GFP (wildtype and L35P mutant) was tested by immunoblotting with anti-GFP antibody, which revealed that the steady-state concentration of the L35P is much lower than that of the corresponding wild-type protein. Porin served as the loading control.

control ATPase ATAD1. We showed that *TbPEX11*-GFP lacking BS2 is mislocalized to mitochondrion in trypanosomes (Figure 3B, lower panel). However, glycosomal targeting also requires the presence of a transmembrane segment for correct targeting. Accordingly, the *TbPEX11* construct containing the first 90 amino acids fused to GFP that lacks the transmembrane domain (TMD) is also mistargeted to mitochondrion. This construct is used here as a control to investigate the requirement for the targeting of *TbPEX11* to mitochondria (Figure 6C, upper panel). Normally, mitochondrial

proteins are targeted via N-terminal or internal mitochondrial targeting signals (Backes et al., 2018; Bykov et al., 2022). After mitochondrial import, the N-terminal targeting presequences of proteins are removed by mitochondrial processing peptidase (MPP) to allow the proper folding of the imported protein (Kunova et al., 2022). Here, we applied the Mitofates webtool to predict putative mitochondrial targeting signals in the N-terminal region of *TbPEX11* (Fukasawa et al., 2015). Although the tool does not identify the *TbPEX11*-NTD as a classical mitochondrial presequence,

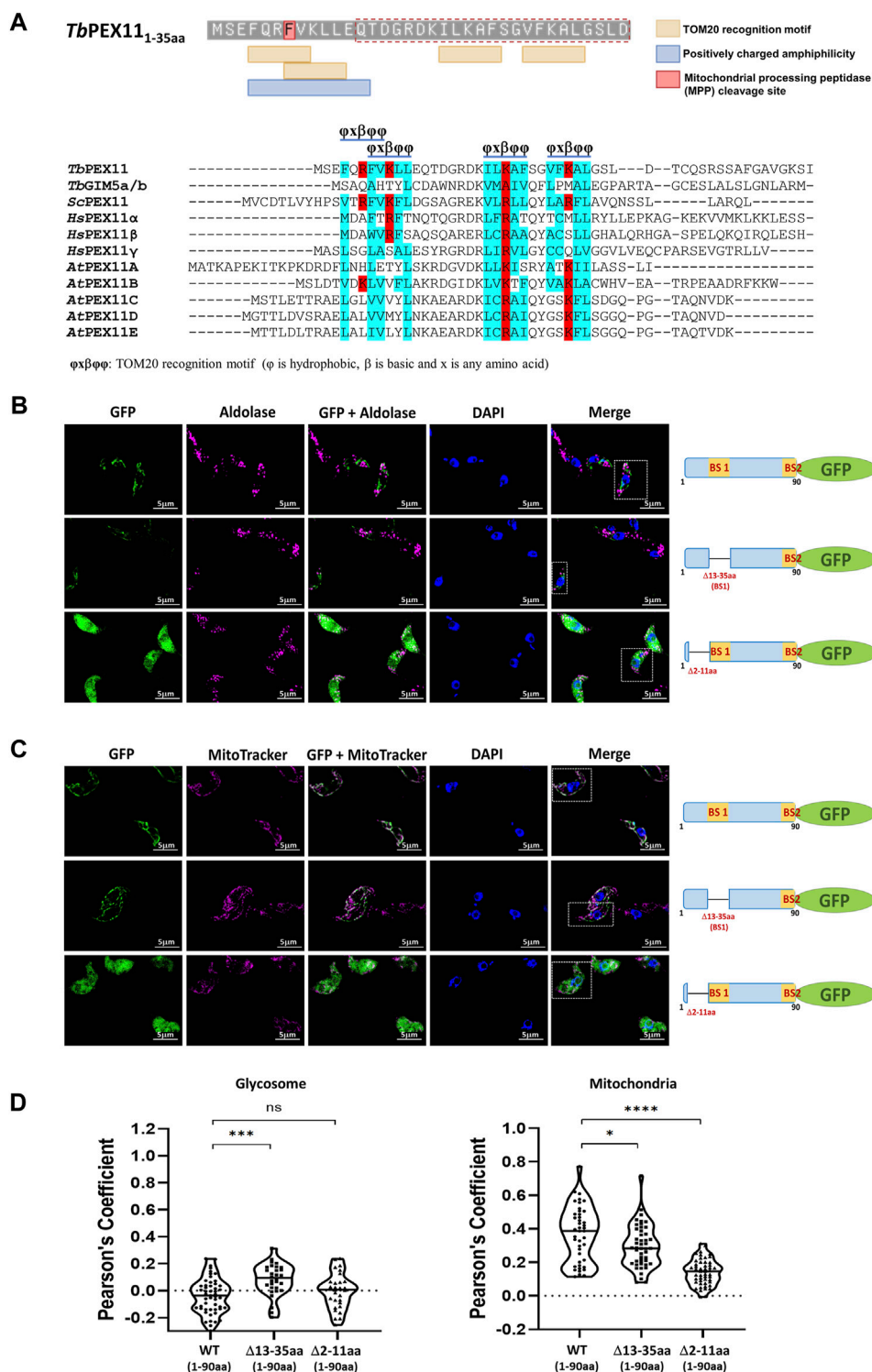


FIGURE 6

Cryptic signal at the N-terminus causes mitochondrial mislocalization of *Tb*PEX11. (A) Upper panel: Prediction of two overlapping putative TOM20 motifs with positively charged amphiphilicity within the N-terminal region *Tb*PEX11 and partially overlapping with the PEX19 binding site region (red dotted box). The residue highlighted in red indicates the presence of a mitochondrial processing peptidase (MPP) cleavage site. The presence of a predicted TOM20 recognition motif and positively charged amphiphilic region with MPP cleavage site were determined by Mitofates webtool (<https://mitf.cbrc.pj.aist.go.jp/MitoFates/cgi-bin/top.cgi>). Lower panel: Multiple sequence alignment of N-terminal sequences of PEX11 proteins from parasites, yeast, humans, and plants indicates the presence of conserved TOM20 motifs with positively charged (red) residues enclosed by hydrophobic (blue) amino acid residues. (B) Subcellular localization of the N-terminal domain of *Tb*PEX11 (1–90aa) fused to GFP with and without deletion of the PEX19-binding site 1 (Δ 13–35aa) or deletion of a N-terminal putative TOM20 binding motif (Δ 2–11aa) by fluorescence and immunofluorescence microscopy. The non-truncated fusion with and without PEX19 binding site 1 (BS1) did not co-localize with the glycosomal marker aldolase but was targeted to mitochondrion as shown below (upper and middle panel). The *Tb*PEX11-GFP lacking the TOM20 motif did mislocalize to the cytosol as (Continued)

FIGURE 6 (Continued)

indicated by the overall cell labelling (lower panel). **(C)** The non-truncated fusion with and without PEX19 binding site 1 (BS1) localized to the mitochondrion, demonstrated by their colocalization with MitoTracker (upper and middle panel, respectively). The glycosomal marker aldolase (pseudo-colored to magenta) was labelled with the corresponding antibody, nuclei and kinetoplasts were stained with DAPI, and mitochondrion was visualized by MitoTracker (pseudo-colored to magenta). Scale bar—5 μm . **(D)** Quantification of the colocalization to glycosomes (left) or the mitochondrion (right). The Pearson's coefficient of colocalization to respective organelle is shown. Dots within the violin plot indicate individual Pearson correlation coefficient data points and the central line represents the median. Statistical significances were calculated by one-way ANOVA, with Dunnett's multiple comparisons test ($n \geq 35$ cells). ****, $p < 0.0001$; ***, $p = 0.0001$; *, $p = 0.0262$; ns, not significant.

it predicts the presence of two tandem TOM20 recognition motifs and a positively charged amphiphilic region with mitochondrial processing peptidase (MPP) cleavage site (Figure 6A, upper panel). The putative TOM20 recognition motifs are in the N-terminal region of *TbPEX11* (4–31 aa), partially overlapping with the identified BS1-binding region for *TbPEX19* (13–35aa) (Figure 6A, upper panel). Further, we looked for the TOM20 motifs by performing multiple sequence alignment of N-terminal region of PEX11 across organisms (Figure 6A, lower panel), which also contains PEX19 binding site (BS) of yeast (Rottensteiner et al., 2004) and the identified PEX19-BS in *T. brucei* and human (this study). This alignment indicates the conservation of TOM20 motifs in the N-terminal region of PEX11, pointing to its role in mitochondrial mislocalization. To test the putative signal sequences for functionality, we analyzed the role of this region for mitochondrial and glycosomal targeting by fluorescence microscopy (Figure 6B). To this end, GFP tagged N-terminal 90 amino acid region of *TbPEX11*, with or without BS1 ($\Delta 13$ -35aa) was analyzed for co-localization with glycosomal marker aldolase (Figure 6B, upper and middle panel). Both fusion proteins were expressed and not targeted to glycosomes but mislocalized to mitochondrion as evident from co-staining with mitochondrial marker (Figure 6C). The expression of these constructs was confirmed by immunoblotting using α -GFP monoclonal antibody (Supplementary Figure S7). Finally, *TbPEX11*_{NTD(1-90aa)}-GFP lacking amino acid residues 2–11, which were predicted to contain TOM20 motifs and positively charged amphiphilicity was analyzed. Expression of this construct did result in a diffuse cytosolic labelling (Figures 6B,C, lower panels), indicating that deletion of this extreme N-terminal region prevented mitochondrial targeting of the fusion protein.

4 Discussion

Here we show that the glycosomal membrane protein *TbPEX11* contains two PEX19 binding sites in its N-terminal region, as shown by peptide array analysis, yeast two-hybrid studies, pull-down experiments, and AlphaScreen assays. PEX19 is a peroxisomal membrane protein (PMP) receptor and chaperone that stabilizes its cargo proteins and targets them to peroxisomes (Hetteema et al., 2000; Sacksteder et al., 2000; Jones et al., 2004). PEX19 binding sites are distributed across the length of cargo proteins, including the C-terminus in case of tail-anchored (TA) proteins (Halbach et al., 2006). Apart from yeast Pex11p (aa 27–41), PEX19 binding sites close to the N-terminus were also found in yeast Pex3p (aa 28–42) and Pxa1p (aa 33–47) (Rottensteiner et al., 2004). Along this line, the N-terminal 95 residues of Pxa1p have recently been shown to be sufficient for targeting a reporter protein to peroxisomes. Interestingly, truncated Pxa1p lacking residues 1–95 still localized to peroxisomes but its

targeting depended on the presence of its interaction partner Pxa2 (Jansen et al., 2023).

Eukaryotic organisms contain multiple proteins belonging to the PEX11 family. In yeast, Pex11p contains a single PEX19-BS near its N-terminus, while in the other ScPEX11-family members, Pex25p and Pex27p, binding of PEX19 occurs far distal from the N-terminus (Rottensteiner et al., 2004). A recent study identified a classical PEX19-BS near the N-terminus of *Pichia pastoris* PEX11 (Zientara-Rytter et al., 2022). However, the study also showed that amphipathic helix 4 (H4) located in the C-terminal region of *PpPEX11*, functions as a second, PEX19-independent mPTS, which is preserved among PEX11-family proteins (Zientara-Rytter et al., 2022). Thus, unlike most PMPs, PEX11 of *Pichia pastoris* can use two mechanisms of transport to peroxisomes, where only one of them depends on its direct interaction with PEX19, but the other does not. The presence of such a PEX19-independent targeting signal is not confirmed in our studies for PEX11 from *T. brucei* and *S. cerevisiae*, as N-terminal mutations or truncations of PEX19-binding sites BS1 or BS2 but not of the amphiphilic helix 4 did prevent efficient glycosomal or peroxisomal targeting of the proteins.

Our data indicate that the N-terminal binding site (BS1) for PEX19 is conserved among *TbPEX11* orthologues but not in PEX11-family member GIM5/B of *Trypanosoma* or *Leishmania* (Saveria et al., 2007). Our results also indicate differences within PEX11 isoforms in humans. All three isoforms, PEX11 α , PEX11 β , and PEX11 γ show sequence similarities to the established PEX19 binding site BS1 in yeast and *T. brucei*, but only HsPEX11 β did bind human PEX19 (Figures 4B,C). PEX11 β is a key factor in the regulation of peroxisome abundance in mammals (reviewed in (Schrader et al., 2016)). It functions as a membrane-remodeling protein that can deform and elongate the peroxisome membrane prior to fission (Delille et al., 2010; Yoshida et al., 2015). Accordingly, PEX11 β is the functional counterpart of yeast and *T. brucei* PEX11 that are targeted to their destination in a PEX19-dependent manner and contribute to the morphogenesis of the peroxisomal membrane, which is required for subsequent fission. Overall, the N-terminal PEX11-binding sites for PEX19 are conserved among species. In this study, this is highlighted by the peptide array analysis of *TbPEX11*, which revealed that human PEX19 binds to the same regions as trypanosomal PEX19 (Supplementary Figure S3).

In the absence of peroxisomes, many PMPs are unstable and degraded or mistargeted to other organelles such as ER and mitochondria. This is seen in yeast as well as in human cells derived from patients suffering from a Peroxisome Biogenesis Disorder (PBD) (Hetteema et al., 2000; Nuebel et al., 2021). In yeast, PEX3 localizes to the ER (Toro et al., 2009), while several peroxins/PMPs including PEX13, PEX14, PEX17 (peroxisomal docking complex) as well as PEX11 and

PEX25 accumulated on mitochondria (Nuebel et al., 2021). Here we show that mislocalization to mitochondria is seen for *Tb*PEX11 lacking its second PEX19-BS and *Sc*PEX11 harboring mutation of its sole PEX19-binding site, (Figure 3B; 5B). Mitochondria have been described as emergency landing places for abandoned peroxins, which results in a partial reconstitution of the peroxisomal import machinery and routing of a substantial part of the peroxisomal proteome to mitochondria (Nuebel et al., 2021; Vogtle and Meisinger, 2021). The mislocalization of PMPs, especially peroxins, to mitochondria are supposed to be the cause for mitochondrial dysfunction in PBD patients (Hettema et al., 2000; Nuebel et al., 2021). Therefore, it is of interest to gain insight into why some PMPs mislocalize to this particular organelle. Mitochondrial targeting signals (MTS) have been extensively characterized across different organisms and consensus motifs can be predicted. Bioinformatic prediction indicated the presence of positively charged amphiphilicity in the extreme N-terminal Helix 1 and detected four TOM20 recognition motifs in NTD of *Tb*PEX11, out of which two tandem motifs coincide with the N-terminal PEX19-BS (Figure 6A). There is no obvious structural similarity between PEX19 and TOM20. The TOM20 recognizes motifs in cargo proteins via its TPR (tetra-ricopeptide repeat) domain, which is not present in PEX19. In our *in vitro* studies, PEX19 can directly interact with the PEX19-BSs, without the requirement of an additional cofactor. Surprisingly, the iMTS-Ls predictor also recognizes PEX19-BSs in *Tb* and *Sc*PEX11 as having Internal Matrix Targeting Signal-like Sequences (iMTSL) propensity (Supplementary Figure S8) (Schneider et al., 2021). How these signals that have primary sequence and potential structural similarities, are faithfully recognized by the correct receptor, and targeted to the correct location requires further investigation. The expression of *Tb*PEX11-NTD lacking N-terminal Helix 1 did not any more mistarget to the mitochondrion. This demonstrates that the N-terminal amphipathic helix at the extreme N-terminus of *Tb*PEX11 is essential for the mitochondrial mislocalization. This result indicates that *Tb*PEX11 harbors a cryptic mitochondrial targeting signal. Whether this is also true for human PEX11 and other PMPs, and involvement of TOM complex machinery requires further investigation.

4.1 What could be the role of a mitochondrial targeting signal of PEX11?

In mature glycosomes/ Peroxisomes of the wild type cells, *Tb*PEX11-NTD is exposed to the cytosol. In this case, the cryptic N-terminal signals may be masked by the oligomerization of PEX11. However, in newly formed glycosomes, which are importing PEX11, these signals may be still accessible to interact with the mitochondrial TOM machinery, and this may mediate glycosome-mitochondrion membrane contact site (MCS). Accordingly, association of *Sc*PEX11 with the mitochondrial TOM complex has been seen in two studies, i) 37-fold enrichment of *Sc*PEX11 in the SILAC based interactome of yeast TOM22 (Opalinski et al., 2018), and ii) interaction of *Sc*PEX11 with TOM22 in split-ubiquitin assay (Eckert and Johnsson, 2003). Recently, a nuclear membrane protein Cnm1 (Contact nucleus mitochondria 1) was shown to interact with TOM70, a component of the mitochondrial TOM (translocase of outer membrane) complex (Eisenberg-Bord et al., 2021). This interaction establishes nuclear-mitochondrial contact sites, which are regulated by

phosphatidylcholine metabolism. Interestingly, Cnm1 harbors two predicted transmembrane domains close to the N-terminus, while C-terminal end contains internal mitochondrial targeting signal-like (iMTS-L) sequences, which are known to directly bind to TOM70 (Backes et al., 2018). Similarly, PEX11 localized to the glycosomal membrane could still associate with the mitochondrial preprotein import machinery to establish glycosome-mitochondrial contact. Interestingly, PEX11 of parasite *Entamoeba histolytica* shows dual localization to peroxisomes and mitosomes (Verner et al., 2021). In baker's yeast, PEX11 interacts with Mdm34, a component of the ER-mitochondria encounter structure (ERMES), and act as a peroxisome-mitochondria tether (Mattiazzi Usaj et al., 2015). It has been shown that a mutant form of Mdm34, a component of the ERMES, which impairs ERMES formation and diminishes its association with the peroxisomal membrane protein PEX11, also causes defects in pexophagy (Liu et al., 2018). Along this line, a role for ERMES complex proteins on regulating peroxisome abundance has been reported (Esposito et al., 2019).

We do not yet know whether the newly identified cryptic mitochondrial targeting signal of *Tb*PEX11 is of functional relevance. However, peroxisomes are not only metabolically linked to mitochondria but also share components of their division machinery (Schrader et al., 2015). These include the tail-anchored adaptor proteins FIS1 and MFF, which are dually targeted to both peroxisomes and mitochondria, where they recruit the fission GTPase DRP1 (also known as DNML1) to the organelle membrane (Schrader et al., 2022). In this context, it is interesting to note that targeting of PEX11 β to mitochondria induces mitochondrial division in human cells. Accordingly, like PEX11 β also *Tb*PEX11 might have the potential to modulate mitochondrial dynamics.

Data availability statement

The original contributions presented in the study are included in the article/Supplementary Material, further inquiries can be directed to the corresponding authors.

Author contributions

CK, VK, and RE conceived and planned the experiments. CK carried out the experiments. NS and KW contributed to the super-resolution fluorescence microscopy. BT performed the AlphaScreen assay. MJ synthesized the peptide array. CK, VK, and RE wrote the manuscript with support from WS. VK and RE supervised the project. All authors contributed to the article and approved the submitted version.

Funding

This project work has received funding from the European Union's Horizon 2020 research and innovation program under the Marie Skłodowska-Curie grant agreement No. 812968—PerICo (to CK, and RE). The work was supported by DFG grant FOR1905 to RE.

Acknowledgments

We thank Paul Michels for kindly providing various antibodies and Wolfgang Girzalsky for critical reading of the manuscript. We acknowledge support by the Open Access Publication Funds of the Ruhr-Universität Bochum.

Conflict of interest

The authors declare that the research was conducted in the absence of any commercial or financial relationships that could be construed as a potential conflict of interest.

References

- Abe, I., and Fujiki, Y. (1998a). cDNA cloning and characterization of a constitutively expressed isoform of the human peroxin Pex11p. *Biochem. Biophys. Res. Commun.* 252 (2), 529–533. doi:10.1006/bbrc.1998.9684
- Abe, I., Okumoto, K., Tamura, S., and Fujiki, Y. (1998b). Clofibrate-inducible, 28-kDa peroxisomal integral membrane protein is encoded by PEX11. *FEBS Lett.* 431 (3), 468–472. doi:10.1016/s0014-5793(98)00815-1
- Agrawal, G., and Subramani, S. (2016). De novo peroxisome biogenesis: evolving concepts and conundrums. *Biochim. Biophys. Acta* 1863 (5), 892–901. doi:10.1016/j.bbamcr.2015.09.014
- Albertini, M., Rehling, P., Erdmann, R., Girzalsky, W., Kiel, J. A., Veenhuis, M., et al. (1997). Pex14p, a peroxisomal membrane protein binding both receptors of the PTS-dependent import pathways. *Cell* 89 (1), 83–92. doi:10.1016/s0092-8674(00)80185-3
- Anton, M., Passreiter, M., Lay, D., Thai, T. P., Gorgas, K., and Just, W. W. (2000). ARF- and coatamer-mediated peroxisomal vesiculation. *Cell Biochem. Biophys.* 32 (1), 27–36. doi:10.1385/cbb:32:1-3:27
- Breidenbach, R. W., and Beevers, H. (1967). Association of the glyoxylate cycle enzymes in a novel subcellular particle from castor bean endosperm. *Biochem. Biophys. Res. Commun.* 27 (4), 462–469. doi:10.1016/s0006-291x(67)80007-x
- Backes, S., Hess, S., Boos, F., Woellhaf, M. W., Godel, S., Jung, M., et al. (2018). Tom70 enhances mitochondrial preprotein import efficiency by binding to internal targeting sequences. *J. Cell Biol.* 217 (4), 1369–1382. doi:10.1083/jcb.201708044
- Baerends, R. J., Faber, K. N., Kiel, J. A., van der Klei, I. J., Harder, W., and Veenhuis, M. (2000). Sorting and function of peroxisomal membrane proteins. *FEMS Microbiol. Rev.* 24 (3), 291–301. doi:10.1111/j.1574-6976.2000.tb00543.x
- Banerjee, S. K., Kessler, P. S., Saveria, T., and Parsons, M. (2005). Identification of trypanosomatid PEX19: functional characterization reveals impact on cell growth and glycosome size and number. *Mol. Biochem. Parasitol.* 142 (1), 47–55. doi:10.1016/j.molbiopara.2005.03.008
- Bonekamp, N. A., Grille, S., Cardoso, M. J., Almeida, M., Aroso, M., Gomes, S., et al. (2013). Self-interaction of human Pex11pβ during peroxisomal growth and division. *PLoS One* 8 (1), e53424. doi:10.1371/journal.pone.0053424
- Boutouja, F., Stiehm, C. M., Mastalski, T., Brinkmeier, R., Reidick, C., El Magraoui, F., et al. (2019). Vps10-mediated targeting of Pep4 determines the activity of the vacuole in a substrate-dependent manner. *Sci. Rep.* 9 (1), 10557. doi:10.1038/s41598-019-47184-7
- Brun, R., and Schonenberger (1979). Cultivation and *in vitro* cloning or procyclic culture forms of *Trypanosoma brucei* in a semi-defined medium. Short communication. *Acta Trop.* 36 (3), 289–292.
- Bykov, Y. S., Flohr, T., Boos, F., Zung, N., Herrmann, J. M., and Schuldiner, M. (2022). Widespread use of unconventional targeting signals in mitochondrial ribosome proteins. *EMBO J.* 41 (1), e109519. doi:10.15252/embj.2021109519
- De Duve, C., and Baudhuin, P. (1966). Peroxisomes (microbodies and related particles). *Physiol. Rev.* 46 (2), 323–357. doi:10.1152/physrev.1966.46.2.323
- Delille, H. K., Agrícola, B., Guimaraes, S. C., Borta, H., Luers, G. H., Fransen, M., et al. (2010). Pex11pβ-mediated growth and division of mammalian peroxisomes follows a maturation pathway. *J. Cell Sci.* 123 (16), 2750–2762. doi:10.1242/jcs.062109
- Eckert, J. H., and Johnsson, N. (2003). Pex10p links the ubiquitin conjugating enzyme Pex4p to the protein import machinery of the peroxisome. *J. Cell Sci.* 116 (17), 3623–3634. doi:10.1242/jcs.00678
- Eisenberg-Bord, M., Zung, N., Collado, J., Drwesh, L., Fenech, E. J., Fadel, A., et al. (2021). Cnm1 mediates nucleus-mitochondria contact site formation in response to phospholipid levels. *J. Cell Biol.* 220 (11), e202104100. doi:10.1083/jcb.202104100
- Erdmann, R., and Blobel, G. (1995). Giant peroxisomes in oleic acid-induced *Saccharomyces cerevisiae* lacking the peroxisomal membrane protein Pmp27p. *J. Cell Biol.* 128 (4), 509–523. doi:10.1083/jcb.128.4.509
- Erdmann, R., and Schliebs, W. (2005). Peroxisomal matrix protein import: the transient pore model. *Nat. Rev. Mol. Cell Biol.* 6 (9), 738–742. doi:10.1038/nrm1710
- Esposito, M., Hermann-Le Denmat, S., and Delahodde, A. (2019). Contribution of ERMES subunits to mature peroxisome abundance. *PLoS One* 14 (3), e0214287. doi:10.1371/journal.pone.0214287
- Faber, K. N., Keizer-Gunnink, I., Pluim, D., Harder, W., Ab, G., and Veenhuis, M. (1995). The N-terminus of amine oxidase of *Hansenula polymorpha* contains a peroxisomal targeting signal. *FEBS Lett.* 357 (2), 115–120. doi:10.1016/0014-5793(94)01317-t
- Fukawasa, Y., Tsuji, J., Fu, S. C., Tomii, K., Horton, P., and Imai, K. (2015). MitoFates: improved prediction of mitochondrial targeting sequences and their cleavage sites. *Mol. Cell Proteomics* 14 (4), 1113–1126. doi:10.1074/mcp.M114.043083
- Galland, N., de Walque, S., Voncken, F. G., Verlinde, C. L., and Michels, P. A. (2010). An internal sequence targets *Trypanosoma brucei* triosephosphate isomerase to glycosomes. *Mol. Biochem. Parasitol.* 171 (1), 45–49. doi:10.1016/j.molbiopara.2010.01.002
- Gao, Y., Skowrya, M. L., Feng, P., and Rapoport, T. A. (2022). Protein import into peroxisomes occurs through a nuclear pore-like phase. *Science* 378 (6625), eadf3971. doi:10.1126/science.adf3971
- Ghaedi, K., Tamura, S., Okumoto, K., Matsuzono, Y., and Fujiki, Y. (2000). The peroxin pex3p initiates membrane assembly in peroxisome biogenesis. *Mol. Biol. Cell* 11 (6), 2085–2102. doi:10.1091/mbc.11.6.2085
- Gietz, R. D., and Woods, R. A. (2002). Transformation of yeast by lithium acetate/single-stranded carrier DNA/polyethylene glycol method. *Methods Enzymol.* 350, 87–96. doi:10.1016/s0076-6879(02)50957-5
- Girzalsky, W., Hoffmann, L. S., Schemenewitz, A., Nolte, A., Kunau, W. H., and Erdmann, R. (2006). Pex19p-dependent targeting of Pex17p, a peripheral component of the peroxisomal protein import machinery. *J. Biol. Chem.* 281 (28), 19417–19425. doi:10.1074/jbc.M603344200
- Goldman, B. M., and Blobel, G. (1978). Biogenesis of peroxisomes: intracellular site of synthesis of catalase and uricase. *Proc. Natl. Acad. Sci. U. S. A.* 75 (10), 5066–5070. doi:10.1073/pnas.75.10.5066
- Gould, S. J., Keller, G. A., Hosken, N., Wilkinson, J., and Subramani, S. (1989). A conserved tripeptide sorts proteins to peroxisomes. *J. Cell Biol.* 108 (5), 1657–1664. doi:10.1083/jcb.108.5.1657
- Halbach, A., Landgraf, C., Lorenzen, S., Rosenkranz, K., Volkmer-Engert, R., Erdmann, R., et al. (2006). Targeting of the tail-anchored peroxisomal membrane proteins PEX26 and PEX15 occurs through C-terminal PEX19-binding sites. *J. Cell Sci.* 119 (12), 2508–2517. doi:10.1242/jcs.02979
- Halbach, A., Lorenzen, S., Landgraf, C., Volkmer-Engert, R., Erdmann, R., and Rottensteiner, H. (2005). Function of the PEX19-binding site of human adrenoleukodystrophy protein as targeting motif in man and yeast. PMP targeting is evolutionarily conserved. *J. Biol. Chem.* 280 (22), 21176–21182. doi:10.1074/jbc.M501750200
- Hasan, S., Platta, H. W., and Erdmann, R. (2013). Import of proteins into the peroxisomal matrix. *Front. Physiol.* 4, 261. doi:10.3389/fphys.2013.00261

Publisher's note

All claims expressed in this article are solely those of the authors and do not necessarily represent those of their affiliated organizations, or those of the publisher, the editors and the reviewers. Any product that may be evaluated in this article, or claim that may be made by its manufacturer, is not guaranteed or endorsed by the publisher.

Supplementary material

The Supplementary Material for this article can be found online at: <https://www.frontiersin.org/articles/10.3389/fcell.2023.1213761/full#supplementary-material>

- Hettema, E. H., Girzalsky, W., van Den Berg, M., Erdmann, R., and Distel, B. (2000). *Saccharomyces cerevisiae* pex3p and pex19p are required for proper localization and stability of peroxisomal membrane proteins. *EMBO J.* 19 (2), 223–233. doi:10.1093/emboj/19.2.223
- Hilpert, K., Winkler, D. F., and Hancock, R. E. (2007). Peptide arrays on cellulose support: sPOT synthesis, a time and cost efficient method for synthesis of large numbers of peptides in a parallel and addressable fashion. *Nat. Protoc.* 2 (6), 1333–1349. doi:10.1038/nprot.2007.160
- Hoepfner, D., Schildknecht, D., Braakman, I., Philippsen, P., and Tabak, H. F. (2005). Contribution of the endoplasmic reticulum to peroxisome formation. *Cell* 122 (1), 85–95. doi:10.1016/j.cell.2005.04.025
- Islinger, M., Li, K. W., Seitz, J., Volkl, A., and Luers, G. H. (2009). Hitchhiking of Cu/Zn superoxide dismutase to peroxisomes—evidence for a natural piggyback import mechanism in mammals. *Traffic* 10 (11), 1711–1721. doi:10.1111/j.1600-0854.2009.00966.x
- Jansen, R. L. M., van den Noort, M., Krikken, A. M., Bibi, C., Bohm, A., Schuldiner, M., et al. (2023). Novel targeting assay uncovers targeting information within peroxisomal ABC transporter Pxa1. *Biochim. Biophys. Acta Mol. Cell Res.* 1870 (5), 119471. doi:10.1016/j.bbamcr.2023.119471
- Jones, J. M., Morrell, J. C., and Gould, S. J. (2004). PEX19 is a predominantly cytosolic chaperone and import receptor for class 1 peroxisomal membrane proteins. *J. Cell Biol.* 164 (1), 57–67. doi:10.1083/jcb.200304111
- Kalel, V. C., and Erdmann, R. (2018). Unraveling of the structure and function of peroxisomal protein import machineries. *Subcell. Biochem.* 89, 299–321. doi:10.1007/978-981-13-2233-4_13
- Kalel, V. C., Schliebs, W., and Erdmann, R. (2015). Identification and functional characterization of Trypanosoma brucei peroxin 16. *Biochim. Biophys. Acta* 1853 (10), 2326–2337. doi:10.1016/j.bbamcr.2015.05.024
- Kall, L., Krogh, A., and Sonnhammer, E. L. (2007). Advantages of combined transmembrane topology and signal peptide prediction—the Phobius web server. *Nucleic Acids Res.* 35, W429–W432. Web Server issue. doi:10.1093/nar/gkm256
- Kamoshita, M., Kumar, R., Anteghini, M., Kunze, M., Islinger, M., Martins Dos Santos, V., et al. (2022). Insights into the peroxisomal protein inventory of zebrafish. *Front. Physiol.* 13, 822509. doi:10.3389/fphys.2022.822509
- Koch, J., Pranjic, K., Huber, A., Ellinger, A., Hartig, A., Kragler, F., et al. (2010). PEX11 family members are membrane elongation factors that coordinate peroxisome proliferation and maintenance. *J. Cell Sci.* 123 (19), 3389–3400. doi:10.1242/jcs.064907
- Krishna, C. K., Franke, L., Erdmann, R., and Kalel, V. C. (2023). “Isolation of glycosomes from trypanosoma brucei,” in *Peroxisomes: Methods and protocols*. Editor M. Schrader (New York, NY: Springer US), 33–45.
- Kunova, N., Havalova, H., Ondrovicova, G., Stojkovicova, B., Bauer, J. A., Bauerova-Hlinkova, V., et al. (2022). Mitochondrial processing peptidases—structure, function and the role in human diseases. *Int. J. Mol. Sci.* 23 (3), 1297. doi:10.3390/ijms23031297
- Kunze, M. (2023). Computational evaluation of peroxisomal targeting signals in metazoa. *Methods Mol. Biol.* 2643, 391–404. doi:10.1007/978-1-0716-3048-8_28
- Kuravi, K., Nagotu, S., Krikken, A. M., Sjollem, K., Deckers, M., Erdmann, R., et al. (2006). Dynamin-related proteins Vps1p and Dnm1p control peroxisome abundance in *Saccharomyces cerevisiae*. *J. Cell Sci.* 119 (19), 3994–4001. doi:10.1242/jcs.031366
- Lazarow, P. B., and Fujiki, Y. (1985). Biogenesis of peroxisomes. *Annu. Rev. Cell Biol.* 1, 489–530. doi:10.1146/annurev.cb.01.110185.002421
- Leon, S., Goodman, J. M., and Subramani, S. (2006). Uniqueness of the mechanism of protein import into the peroxisome matrix: transport of folded, co-factor-bound and oligomeric proteins by shuttling receptors. *Biochim. Biophys. Acta* 1763 (12), 1552–1564. doi:10.1016/j.bbamcr.2006.08.037
- Li, X., and Gould, S. J. (2002). PEX11 promotes peroxisome division independently of peroxisome metabolism. *J. Cell Biol.* 156 (4), 643–651. doi:10.1083/jcb.200112028
- Lingard, M. J., and Trelease, R. N. (2006). Five Arabidopsis peroxin 11 homologs individually promote peroxisome elongation, duplication or aggregation. *J. Cell Sci.* 119 (9), 1961–1972. doi:10.1242/jcs.02904
- Liu, X., Wen, X., and Klionsky, D. J. (2018). Endoplasmic reticulum—mitochondria contacts are required for pexophagy in *Saccharomyces cerevisiae*. *Contact* 2, 2158. *Thousand Oaks* 2. doi:10.1177/2515256418821584
- Lorenz, P., Maier, A. G., Baumgart, E., Erdmann, R., and Clayton, C. (1998). Elongation and clustering of glycosomes in Trypanosoma brucei overexpressing the glycosomal Pex11p. *EMBO J.* 17 (13), 3542–3555. doi:10.1093/emboj/17.13.3542
- Maier, A., Lorenz, P., Voncken, F., and Clayton, C. (2001). An essential dimeric membrane protein of trypanosome glycosomes. *Mol. Microbiol.* 39 (6), 1443–1451. doi:10.1046/j.1365-2958.2001.02333.x
- Marshall, P. A., Dyer, J. M., Quick, M. E., and Goodman, J. M. (1996). Redox-sensitive homodimerization of Pex11p: a proposed mechanism to regulate peroxisomal division. *J. Cell Biol.* 135 (1), 123–137. doi:10.1083/jcb.135.1.123
- Mattiazzi Usaj, M., Brloznik, M., Kaferle, P., Zitnik, M., Wolinski, H., Leitner, F., et al. (2015). Genome-wide localization study of yeast Pex11 identifies peroxisome-mitochondria interactions through the ERMES complex. *J. Mol. Biol.* 427 (11), 2072–2087. doi:10.1016/j.jmb.2015.03.004
- Mayerhofer, P. U. (2016). Targeting and insertion of peroxisomal membrane proteins: eR trafficking versus direct delivery to peroxisomes. *Biochim. Biophys. Acta* 1863 (5), 870–880. doi:10.1016/j.bbamcr.2015.09.021
- McNew, J. A., and Goodman, J. M. (1994). An oligomeric protein is imported into peroxisomes *in vivo*. *J. Cell Biol.* 127 (5), 1245–1257. doi:10.1083/jcb.127.5.1245
- Meinecke, M., Bartsch, P., and Wagner, R. (2016). Peroxisomal protein import pores. *Biochim. Biophys. Acta* 1863 (5), 821–827. doi:10.1016/j.bbamcr.2015.10.013
- Motley, A. M., and Hettema, E. H. (2007). Yeast peroxisomes multiply by growth and division. *J. Cell Biol.* 178 (3), 399–410. doi:10.1083/jcb.200702167
- Moyersoen, J., Choe, J., Fan, E., Hol, W. G., and Michels, P. A. (2004). Biogenesis of peroxisomes and glycosomes: trypanosomatid glycosome assembly is a promising new drug target. *FEMS Microbiol. Rev.* 28 (5), 603–643. doi:10.1016/j.femsre.2004.06.004
- Murphy, M. A., Phillipson, B. A., Baker, A., and Mullen, R. T. (2003). Characterization of the targeting signal of the Arabidopsis 22-kD integral peroxisomal membrane protein. *Plant Physiol.* 133 (2), 813–828. doi:10.1104/pp.103.027870
- Neuhauser, A., Kooshapur, H., Wolf, J., Meyer, N. H., Madl, T., Saidowsky, J., et al. (2014). A novel Pex14 protein-interacting site of human Pex5 is critical for matrix protein import into peroxisomes. *J. Biol. Chem.* 289 (1), 437–448. doi:10.1074/jbc.M113.499707
- Nuebel, E., Morgan, J. T., Fogarty, S., Winter, J. M., Lettlova, S., Berg, J. A., et al. (2021). The biochemical basis of mitochondrial dysfunction in Zellweger Spectrum Disorder. *EMBO Rep.* 22 (10), e51991. doi:10.15252/embr.202051991
- Opalinski, L., Song, J., Priesnitz, C., Wenz, L. S., Oeljeklaus, S., Warscheid, B., et al. (2018). Recruitment of cytosolic J-proteins by TOM receptors promotes mitochondrial protein biogenesis. *Cell Rep.* 25 (8), 2036–2043.e5. doi:10.1016/j.celrep.2018.10.083
- Opperdoes, F. R., and Borst, P. (1977). Localization of nine glycolytic enzymes in a microbody-like organelle in trypanosoma brucei: the glycosome. *FEBS Lett.* 80 (2), 360–364. doi:10.1016/0014-5793(77)80476-6
- Orth, T., Reumann, S., Zhang, X., Fan, J., Wenzel, D., Quan, S., et al. (2007). The PEROXIN11 protein family controls peroxisome proliferation in Arabidopsis. *Plant Cell* 19 (1), 333–350. doi:10.1105/tpc.106.045831
- Platta, H. W., Girzalsky, W., and Erdmann, R. (2004). Ubiquitination of the peroxisomal import receptor Pex5p. *Biochem. J.* 384 (1), 37–45. doi:10.1042/BJ20040572
- Platta, H. W., Grunau, S., Rosenkranz, K., Girzalsky, W., and Erdmann, R. (2005). Functional role of the AAA peroxins in dislocation of the cycling PTS1 receptor back to the cytosol. *Nat. Cell Biol.* 7 (8), 817–822. doi:10.1038/ncb1281
- Reichle, R. E., and Alexander, J. V. (1965). Multiperforate septations, Woronin bodies, and septal plugs in Fusarium. *J. Cell Biol.* 24 (3), 489–496. doi:10.1083/jcb.24.3.489
- Rhodin, J. (1954). “Correlation of ultrastructural organization: and function in normal and experimentally changed proximal convoluted tubule cells of the mouse kidney: an electron microscopic study,” (Sweden: Dept. of Anatomy, Karolinska Institutet), PhD Thesis.
- Rottensteiner, H., Kramer, A., Lorenzen, S., Stein, K., Landgraf, C., Volkmer-Engert, R., et al. (2004). Peroxisomal membrane proteins contain common Pex19p-binding sites that are an integral part of their targeting signals. *Mol. Biol. Cell* 15 (7), 3406–3417. doi:10.1091/mbc.e04-03-0188
- Rottensteiner, H., Stein, K., Sonnenhol, E., and Erdmann, R. (2003). Conserved function of pex11p and the novel pex25p and pex27p in peroxisome biogenesis. *Mol. Biol. Cell* 14 (10), 4316–4328. doi:10.1091/mbc.e03-03-0153
- Rucktaschel, R., Thoms, S., Sidorovitch, V., Halbach, A., Pechlivanis, M., Volkmer, R., et al. (2009). Farnesylation of pex19p is required for its structural integrity and function in peroxisome biogenesis. *J. Biol. Chem.* 284 (31), 20885–20896. doi:10.1074/jbc.M109.016584
- Sacksteder, K. A., Jones, J. M., South, S. T., Li, X., Liu, Y., and Gould, S. J. (2000). PEX19 binds multiple peroxisomal membrane proteins, is predominantly cytoplasmic, and is required for peroxisome membrane synthesis. *J. Cell Biol.* 148 (5), 931–944. doi:10.1083/jcb.148.5.931
- Saveria, T., Halbach, A., Erdmann, R., Volkmer-Engert, R., Landgraf, C., Rottensteiner, H., et al. (2007). Conservation of PEX19-binding motifs required for protein targeting to mammalian peroxisomal and trypanosome glycosomal membranes. *Eukaryot. Cell* 6 (8), 1439–1449. doi:10.1128/EC.00084-07
- Schneider, K., Zimmer, D., Nielsen, H., Herrmann, J. M., and Muhlhaus, T. (2021). iMLP, a predictor for internal matrix targeting-like sequences in mitochondrial proteins. *Biol. Chem.* 402 (8), 937–943. doi:10.1515/hsz-2021-0185
- Schrader, M., Costello, J., Godinho, L. F., and Islinger, M. (2015). Peroxisome-mitochondria interplay and disease. *J. Inher. Metab. Dis.* 38 (4), 681–702. doi:10.1007/s10545-015-9819-7
- Schrader, M., Costello, J. L., Godinho, L. F., Azadi, A. S., and Islinger, M. (2016). Proliferation and fission of peroxisomes - an update. *Biochim. Biophys. Acta* 1863 (5), 971–983. doi:10.1016/j.bbamcr.2015.09.024

- Schrader, M., Reuber, B. E., Morrell, J. C., Jimenez-Sanchez, G., Obie, C., Stroh, T. A., et al. (1998). Expression of PEX11beta mediates peroxisome proliferation in the absence of extracellular stimuli. *J. Biol. Chem.* 273 (45), 29607–29614. doi:10.1074/jbc.273.45.29607
- Schrader, T. A., Carmichael, R. E., Islinger, M., Costello, J. L., Hacker, C., Bonekamp, N. A., et al. (2022). PEX11 β and FIS1 cooperate in peroxisome division independently of mitochondrial fission factor. *J. Cell Sci.* 135 (13), jcs259924. doi:10.1242/jcs.259924
- South, S. T., and Gould, S. J. (1999). Peroxisome synthesis in the absence of preexisting peroxisomes. *J. Cell Biol.* 144 (2), 255–266. doi:10.1083/jcb.144.2.255
- Sulter, G. J., Verheyden, K., Mannaerts, G., Harder, W., and Veenhuis, M. (1993). The *in vitro* permeability of yeast peroxisomal membranes is caused by a 31 kDa integral membrane protein. *Yeast* 9 (7), 733–742. doi:10.1002/yea.320090707
- Swinkels, B. W., Gould, S. J., Bodnar, A. G., Rachubinski, R. A., and Subramani, S. (1991). A novel, cleavable peroxisomal targeting signal at the amino-terminus of the rat 3-ketoacyl-CoA thiolase. *EMBO J.* 10 (11), 3255–3262. doi:10.1002/j.1460-2075.1991.tb04889.x
- Tam, Y. Y., Torres-Guzman, J. C., Vizeacoumar, F. J., Smith, J. J., Marelli, M., Aitchison, J. D., et al. (2003). Pex11-related proteins in peroxisome dynamics: a role for the novel peroxin Pex27p in controlling peroxisome size and number in *Saccharomyces cerevisiae*. *Mol. Biol. Cell* 14 (10), 4089–4102. doi:10.1091/mbc.e03-03-0150
- Thoms, S., and Gartner, J. (2012). First PEX11 β patient extends spectrum of peroxisomal biogenesis disorder phenotypes. *J. Med. Genet.* 49 (5), 314–316. doi:10.1136/jmedgenet-2012-100899
- Toro, A. A., Araya, C. A., Cordova, G. J., Arredondo, C. A., Cardenas, H. G., Moreno, R. E., et al. (2009). Pex3p-dependent peroxisomal biogenesis initiates in the endoplasmic reticulum of human fibroblasts. *J. Cell Biochem.* 107 (6), 1083–1096. doi:10.1002/jcb.22210
- Tyler, K. M., Matthews, K. R., and Gull, K. (2001). Anisomorphic cell division by African trypanosomes. *Protist* 152 (4), 367–378. doi:10.1078/1434-4610-00074
- Van Ael, E., and Franssen, M. (2006). Targeting signals in peroxisomal membrane proteins. *Biochim. Biophys. Acta* 1763 (12), 1629–1638. doi:10.1016/j.bbamcr.2006.08.020
- van Roermund, C. W., Tabak, H. F., van Den Berg, M., Wanders, R. J., and Hettema, E. H. (2000). Pex11p plays a primary role in medium-chain fatty acid oxidation, a process that affects peroxisome number and size in *Saccharomyces cerevisiae*. *J. Cell Biol.* 150 (3), 489–498. doi:10.1083/jcb.150.3.489
- Verner, Z., Zarsky, V., Le, T., Narayanasamy, R. K., Rada, P., Rozbesky, D., et al. (2021). Anaerobic peroxisomes in *Entamoeba histolytica* metabolize myo-inositol. *PLoS Pathog.* 17 (11), e1010041. doi:10.1371/journal.ppat.1010041
- Vogtle, F. N., and Meisinger, C. (2021). Mitochondria as emergency landing for abandoned peroxins. *EMBO Rep.* 22 (10), e53790. doi:10.15252/embr.202153790
- Voncken, F., van Hellemond, J. J., Pfisterer, I., Maier, A., Hillmer, S., and Clayton, C. (2003). Depletion of GLM5 causes cellular fragility, a decreased glycosome number, and reduced levels of ether-linked phospholipids in trypanosomes. *J. Biol. Chem.* 278 (37), 35299–35310. doi:10.1074/jbc.M301811200
- Yoshida, Y., Niwa, H., Honsho, M., Itoyama, A., and Fujiki, Y. (2015). Pex11 mediates peroxisomal proliferation by promoting deformation of the lipid membrane. *Biol. Open* 4 (6), 710–721. doi:10.1242/bio.201410801
- Zientara-Rytter, K. M., Mahalingam, S. S., Farre, J. C., Carolino, K., and Subramani, S. (2022). Recognition and chaperoning by Pex19, followed by trafficking and membrane insertion of the peroxisome proliferation protein, Pex11. *Cells* 11 (1), 157. doi:10.3390/cells11010157